IMPROVEMENT OF CUSTOMER BASELINE CALCULATION METHODOLOGIES OF DEMAND RESPONSE USING MAXIMAL OVERLAP DISCRETE WAVELET PACKET TRANSFORM

by

Johnson Opadere

A thesis submitted to the faculty of
The University of North Carolina at Charlotte
in partial fulfillment of the requirements
for the degree of Master of Science in
Economics

Charlotte

2020

Approved by:

_____

Dr. Peter Schwarz

_____

Dr. Valentina Cecchi

_____

Dr. Paul Gaggl

ABSTRACT

JOHNSON OPADERE. Improvement of Customer Baseline Calculation Methodologies of Demand Response using Maximal Overlap Discrete Wavelet Packet Transform. (Under the direction of DR. PETER SCHWARZ)

Demand response is a reduction in electricity consumption designed to prevent system emergencies stemming from demand spikes during peak periods. While demand response has been embraced as a cheaper alternative than adding peaking generation, the implementation has been challenging, especially for residential customers. The peak period baseline load of residential customers is difficult to estimate due to the load pattern randomness emanating from weather or behavioral variations. In this thesis, a novel clustering-based customer baseline load (CBL) is proposed to improve the error performance of the traditional baseline estimation methods. The proposed method assumes there are true underlying clusters of consumption profiles of residential customers, which differ only with respect to some feature(s). The spectral features obtained, via Shannon entropy (SE) estimates, from maximal overlap discrete wavelet packet transform (MODWPT) decomposition of the historical consumption, were harnessed to compute a set of new CBLs for existing baseline methods. The proposed method shows significant error performance improvement with respect to peak period baselines. The thesis is extended to a case study of a Dynamic Peak Rebate (DPR) pricing demand response program. The amount of rebate payment was estimated by clustered linear regression (CLR). Finally, the demand reduction costs of the DR event load reduction are calculated for various CBL estimation methods. The proposed CBL method comparatively provides the lowest demand reduction costs in all the DR events considered.

ACKNOWLEDGMENTS

My deepest gratitude goes to my advisor Dr. Peter Schwarz, who expertly guided me throughout the research and writing of this thesis. This feat would not have been possible without his invaluable suggestions, support, and encouragement.

I am extremely grateful to Dr. Valentina Cecchi and Dr. Paul Gaggl for serving as the thesis committee members and for painstakingly correcting and improving this work.

My profound appreciation also goes to Dr. Craig Depken II and Ms. Amy Riter. They patiently guided, supported, and advised me throughout the master's program.

I am indebted to the professors who have taught and guided me during my master's program in classes and projects: Dr. Dmitry Shapiro, Dr. Lisa Schulkind, Dr. Hwan C. Lin, Dr. Azhar Iqbar, and many others. I sincerely thank Dr. Saeed Mohajeryami, whose research provided a very valuable background for this work.

Many thanks to my beautiful wife, Dianarose, and cute daughter, Zuri, for their understanding when I needed to spend more time on this research work than I spent with them. Finally, I thank my mother and the entire Opadere family for their unending moral support, encouragement, and prayers.

TABLE OF CONTENTS

LIST OF TABLES

LIST OF FIGURES

CHAPTER 1: INTRODUCTION

1.1 Introduction

Demand response (DR) enables electricity consumers to significantly contribute to the operation of the electric grid by optimizing its electricity usage in response to time-based or incentive-based rates. The customers respond by either reducing or shifting their energy consumption. The response has the capability of averting the cost of peaking generators and eliminating blackouts [1]. DR is usually implemented through programs facilitated by utility companies and aggregators as well as government [2] as resource options for balancing supply and demand. Moreover, the DR program savings from the avoidance of the cost of incurring new peaking capacity can be significant, in addition to the savings from peak period energy cost. For example, in the US alone, a five percent peak time rebate (PTR) via DR programs over 20 years is estimated to yield a savings of up to $35 billion [3].

The most commonly utilized demand response program mechanisms are the Direct Load Control (DLC) such as in [4, 5, 6], and price-based programs [7]. The DLC programs allow a utility or an aggregator (DR operator) to directly alter or time-shift a customer's consumption via remote control switches. The targeted consumer loads in DLC are mainly air conditioners, but electric water heaters and pool pumps can also be included [8]. The limitation of the DLC programs is the low degree of trust the customers have in surrendering the direct control of their equipment to the utilities [9]. In addition, centralized controlling of the remote devices installed on customers' sites could be cumbersome as the size of the participants gets large [4].

In price-based programs, customers are incentivized, usually with time-based rates or a rebate, to adjust their consumption during peak periods [6]. Price-based rates

can be broadly categorized into time-of-use pricing (TOU) and dynamic pricing. A TOU pricing plan divides the day into intervals with fixed retail prices regardless of system conditions. Since prices are fixed in the intervals regardless of the system conditions (wholesale price availability or stressed system), customers are not motivated to reduce demand based on real-time conditions with a TOU pricing plan.

Dynamic pricing plans entail charging varying prices in response to system conditions. The price variation encourages the customers to reduce their demand with wholesale price offers or a stressed system condition. The common plans under dynamic pricing include real-time pricing (RTP), critical peak pricing (CPP), and critical peak rebates (CPR). In the case study DR programs employed in this thesis, the CPP and CPR are referred to as dynamic peak pricing (DPP) and dynamic peak rebate (DPR), respectively, following the data source program report [10]. Since the terms are essentially the same [11], I use DPP and DPR to refer to CPP and CPR, respectively, for the rest of this thesis.

The strategies proposed and the DR events used in this thesis are for the DPR pricing plan. According to behavioral science theory, people always have a stronger preference to avoid losses than to acquire gains. The same applies to electricity dynamic pricing plans, where there is a higher likelihood of customers subscribing to DPR than DPP DR programs [8]. The particular focus of the thesis as regards DPR DR programs is on the estimation of customer baseline load (CBL), and the impact of the CBL accuracy on the demand reduction costs of the load reduction in the peak periods.

A novel clustering-based CBL estimation method is proposed in this thesis with the view to improving the accuracy of the customer baselines. In addition, the rebate payment of actual DPR events is estimated using clustered linear regression. With the estimated rebate, comparative evaluation of the demand reduction costs of the DR programs, using the proposed CBL method and the existing methods, are presented.

Since one of the objectives of a DR operator is to motivate the consumers to reduce their electricity usage during peak periods, the utility or the operator is required to estimate the customer baseline (CBL) for the event period. The CBL enables the operator to compute a customer's load reduction during the event period, and to gain insights into the customer's incentive for participating in the DR program [12].

1.2   Motivation

Accurate estimation of CBL is a key element in the successful realization of the objectives of DR. The CBL of residential customers is particularly challenging to estimate due to the randomness in the load pattern emanating from weather or behavioral variations.

There is an adverse consequence from an underestimation or overestimation of CBL, especially in a rebate based DR program. With inaccurate baselines, the appropriate rebate will not be paid to the customers. CBL underestimation results in under-calculated peak time actual load reduction resulting in an underpayment of rebate. Ultimately, the motivations of the customers to participate in the DR program will diminish. Such customers may even consider canceling the contract or refuse to participate in subsequent DR programs. On the other hand, overestimation of CBL makes the DR operator overpay rebate. And overpayment of incentive can lead to a decrease in motivation for the operator to continue the program [13].

Since there is still no universally accepted method for computing CBL, it is up to DR operators to develop or apply a suitable CBL estimation method for their customers. For instance, California Independent System Operator (CAISO), New York ISO (NYISO), Pennsylvania Jersey Maryland Power Pool (PJM), and ISONE are known to have employed CBL averaging methods. The averaging methods are of different types and more explicitly discussed in Chapter 2. The main demerit of the averaging methods is their vulnerability to significant errors when dealing with

residential customers.

Recently, a machine learning technique called clustering is gaining popularity for estimating CBL of residential customers. [7, 14, 15, 16]. Clustering undermines the strategic behavior of customers to inflate rebates. If CBLs are based on individual customer demands, and if customers know the dates and hours the utility is using to determine the baseline, they can artificially inflate their usage by turning on appliances or increasing the intensity of use above what they would ordinarily choose. If their CBL is based upon a cluster of customers, the individual's action will only have a small effect on that customer's baseline[17, 18]. Authors in [7, 14] show their proposed discrete Fourier transform (DFT) based clustering CBL methods have significantly better accuracy than the averaging methods. However, the existing clustering CBL methods are vulnerable to errors and instability due to sensitivity to the starting point of the employed consumption time-series data.

In this thesis, I leverage the characteristics of maximal overlap discrete wavelet packet transform, whose decomposition is not sensitive to the starting point of the time-series data [19], to extract clustering features for consumption profiles of residential customers. The proposed method in this work is robust to the mentioned drawback of the existing clustering-based method methods.

1.3   Contribution of the Thesis

In this thesis, I show the effectiveness of clustering-based strategies in the reduction of randomness, causing inaccuracy of the conventional CBL estimation methods. In particular, with the integration of the novel maximal overlap discrete wavelet packet transform decomposition-based technique with the existing CBL estimation methods, the accuracy of the resultant baselines are improved considerably. The performance is evaluated with dynamic peak rebate (DPR) structure DR programs.

This thesis further exposes the effect of CBL estimation accuracy on the demand reduction costs of the load reduction in a DPR demand response event. The principal

contributions of this thesis are:

- I propose a novel clustering-based CBL estimation method, which leverages the entropy features obtained from maximal overlap discrete wavelet packet transform (MODWPT). The proposed method shows the overall highest CBL estimation accuracy as compared to all the benchmark techniques.

- Unlike in most studies where the data used are not from a real-world DR program, I evaluate the performance of the proposed method and the benchmarks with data from an actual dynamic peak rebate program. Using the estimated load impact from an actual DR program, I evaluate the baseline error performance and rebate payment errors from using various CBL methods.

- I leverage the clustered linear regression (CLR) to deduce the amount of rebate paid to customers, in a dynamic peak rebate DR program, for evaluation of program-level demand reduction cost.

- The DFT-based method is used as the representative of the existing clustering methods in this work. When proposed in [7, 14], the DFT-based method's accuracy was evaluated using data that are not from actual DR programs. In this thesis, I implemented the estimation technique, and its evaluation shows a significantly better performance than the conventional methods. Although the performance of the DFT-based clustering is somewhat comparable to the proposed method in this thesis, the accuracy of the latter outperforms the former in all the DR events evaluated.

- Finally, I present a program-level evaluation of the rebate payment in order to determine the associated cost of load reduction during DR events. The obtained results are presented as the demand reduction costs of the dynamic peak rebate demand reduction, whose values depend on the employed CBL method.

1.4   Organization of the Thesis

This work is subsequently organized as follows.

- Chapter 2 reviews the existing CBL estimation methods. The formulas, the eligible days, and discussions of each conventional baseline method are presented. Also reviewed is the DFT-based clustering baseline estimation method.

- Chapter 3 introduces the novel clustering-based baseline method proposed in this thesis. Wavelet energy and entropy features extraction from maximal overlap discrete wavelet transform decomposition is described. The clustering of the participating customers based on wavelet entropy features is also discussed.

- Chapter 4 presents the case study DR programs with which the existing and the proposed CBL estimation techniques are evaluated.

- Chapter 5 focuses on the estimation of the rebate amount paid to customers in the case study DR programs of Chapter 4. In this chapter, I apply clustered linear regression to estimates the amount of rebate from the actual event rebate payment for the peak time load reduction in the DR program.

- Chapter 6 describes the implementation of the proposed baseline estimation method using the datasets from the case study programs. The results are presented using the CBL accuracy metrics. Rebate payment errors and demand reduction costs of the load reduction during the DR events, for the considered CBL methods, are also presented.

- Finally, Chapter 7 concludes this thesis. The chapter points out that the proposed CBL method outperforms all the benchmark methods in all the considered DR events. The superior performance of demand reduction costs of the peak time load reduction of the proposed method over the benchmarks is also discussed.

CHAPTER 2: OVERVIEW OF CBL ESTIMATION METHODS

This chapter presents an overview of the conventional CBL estimation methods and an existing clustering-based technique. First, I present the terms in the CBL models.

Consider a set of customers subscribed to a specified DR program event. The set of customers is indexed by $\mathcal{I} = \{1, 2, \cdots, I\}$. Let the energy consumption measured by the smart metering device on day d at timeslot t be denoted by $L_i(d, t)$. To distinguish between the daily measurement horizon and that of the DR event period, I represent the daily consumption measurement set by $\mathcal{T} = \{1, 2, \cdots, T\}$, in which $t \in \mathcal{T}$. The peak period on an event day d is depicted by $\mathcal{P} = \{1, 2, \cdots, P\}$, where $\mathcal{P} \subset \mathcal{T}$.

Many CBL estimation methods are employed in practice. The literature is also being updated with new methods in a bid to provide better accuracy than the existing ones. The existing baseline methods include LowXofY, MidXofY, HighXofY, exponential moving average (EMA), and regression. The methods are reviewed and employed as benchmarks in this work. With the recent trend of utilizing machine learning (ML) approaches to improve accuracy in estimation theory and predictive modeling, there is an advent of the application of various ML algorithms to CBL estimation in recent literature. One of the ML-based CBL estimation methods, with significantly better error performance over the existing methods, is the Discrete Fourier Transform (DFT)-based clustering [7, 14]. The DFT-based Clustering method is reviewed and also added to the benchmarks in this work.

I define an *eligible day* as a type of days counted during the non-DR days, which is used to calculate the CBL. For simple averaging methods (LowXofY, MidXofY,

and HighXofY), EMA and regression, weekdays, non-holiday days, and non-past DR event days are the eligible days preceding the actual DR event day for computing the CBL baseline. I depict the set of eligible days for customer i participating in a DR on event day d as $\mathcal{D}_e^i$.

2.1 LowXofY

LowXofY is one of the averaging methods for CBL estimation. The CBL is computed as the arithmetic mean of the consumption from the lowest X days of the Y eligible days preceding the DR event day d, where X $\leq$ Y and Y $\leq \mathcal{D}_e$. I define the LowXofY days of customer i preceding the DR event day d as $Low(X, Y, d) \subseteq \mathcal{D}_e^i$. Therefore, the LowXofY CBL of customer i for time slot $t \subset \mathcal{T}$ on the event day d is computed as

$$\text{CBL}_i(d, t) = \frac{1}{X} \sum_{d \in Low(X,Y,d)} L_i(d, t). \tag{2.1}$$

In this paper, I use Low4of5 as one of the benchmark CBL estimation methods.

2.2 MidXofY

MidXofY CBL estimation method makes use of X middle days of the Y days of the eligible days preceding the DR event day d to compute the CBL. To determine the middle X days out of the Y eligible days, a particular number, denoted by Z, of the lowest day(s) and highest day(s) are dropped. Given X $\leq$ Y and Y $\leq \mathcal{D}_e$, $Z = (Y - X)/2$. It is required for Z to be an integer, hence $(Y - X)\text{mod}2 = 0$. The MidXofY CBL of customer i for the time $t \subset \mathcal{T}$ on the event day d can be expressed as

$$\text{CBL}_i(d, t) = \frac{1}{X} \sum_{d \in Mid(X,Y,d)} L_i(d, t), \tag{2.2}$$

where $Mid(X, Y, d)$ is the MidXofY days of customer i preceding the DR event day d. I adopt the Mid4of6 in this research as one of the conventional baseline methods.

2.3   HighXofY

HighXofY is the opposite of LowXofY. The highest X days of the Y of the eligible days denoted by $High(X, Y, d)$, preceding the DR event day d, are used in computing the CBL. $X \leq Y$ and $Y \leq \mathcal{D}_e$. The HighXofY CBL is the arithmetic mean of the energy consumption in the selected X days. The HighXofY CBL the customer for time slot $t \subset \mathcal{T}$ on the event day d is computed as

$$\text{CBL}_i(d, t) = \frac{1}{X} \sum_{d \in High(X,Y,d)} L_i(d, t). \tag{2.3}$$

HighXofY CBL estimation method is popularly used by many utility company and ISOs, such as SDGE (High3of5), Ontario (High4of5), PJM (High3of10), New York ISO (High5of10), and PowerCents DC (High3of20, High5of20, High10of20) [20]. The High5of10 is included in the CBL estimation methods employed in this work.

2.4   Exponential Moving Average

Exponential Moving Average (EMA), unlike the other averaging CBL estimation methods, uses weighted average of a customer's historical consumption. The weight decreases exponentially with time. The days that make up the historical load data, from the measurement start day up to the day before the DR event day d, are all eligible days.

Let $M = \{m_1, \cdots, m_K\}$ be the measurement days (all eligible), and the last measurement day is the day before the event day, that is $m_K = d - 1$. If $1 \leq \tau \leq k$ is defined as a constant, the initial average consumption customer i at timeslot t can be expressed as

$$v_i(m_\tau, t) = \frac{1}{\tau} \sum_{k=1}^{\tau} L_i(m_k, t). \tag{2.4}$$

Furthermore, the EMA for $\tau < k \leq K$ is

$$v_i(m_k, t) = (\lambda \cdot v_i(m_{k-1}, t)) + ((1 - \lambda) \cdot L_i(m_k, t)), \qquad (2.5)$$

where $\lambda \in [0, 1]$. Thus, the EMA CBL of customer i at timeslot t on the DR event day is computed as

$$\text{CBL}_i(d, t) = v_i(m_K, t). \qquad (2.6)$$

The λ value of 0.9 is adopted in this work, which means a weight of 10% is put on the current day and 90% is put on the previous day. The idea of apportioning more weight to the previous day than the current is to reduce the possibility of customers to "game" the DR program [21].

2.5   Regression

This method employs regression to estimate a customer's baseline for a DR event day. Consumption data from historical eligible days are used for determine the regression parameters for the event day d CBL computation. The regression method CBL customer i for time slot $t \subset \mathcal{T}$ on the event day d is stated as

$$\text{CBL}_i(d, t) = \left(\boldsymbol{\beta}_{i,t}\right)^\top \boldsymbol{x}_{i,t} + \epsilon_{i,t}, \qquad (2.7)$$

where $\boldsymbol{x}_{i,t}$ is the feature vector, $\boldsymbol{\beta}_{i,t}$ is the regression coefficient vector, and $\epsilon_{i,t}$ is the error term. $\boldsymbol{x}_{i,t}$ consists of explanatory variables such as the historical consumption, weather variables (e.g temperature, humidity) or daylight variables (e.g sunrise and sunset time). However, since the datasets made available for the events considered in this thesis do not include weather and daylight measurement, I follow the approach of [12] to constitute the feature vector with the historical consumption.

2.6   DFT-based Clustering

DFT Clustering is the representative machine learning technique considered in this work. Authors in [22] proposed transforming the historical consumption time domain data into the frequency domain using Discrete Fourier Transform (DFT). The objective of the transformation is to separate high frequency and low-frequency components.

The frequency components are separated using low-pass and high-pass filters. The former isolates the low-frequency component of the signal, and the latter allows only the high-frequency. Both filters are designed with a cut-off frequency as a threshold for attenuating undesired frequencies. Each separated frequency component is reconstructible into a corresponding low or high-frequency portion of the original time-domain signal. An index called *predictability index* is computed by subtracting the ratio of the sum of the absolute values of the reconstructed high frequency portion s_i^{hf} of the signal to the sum of the original time-domain signal s_i from one. That is,

$$P_{index} = 1 - \frac{\sum_{i=1}^{I} \left| s_i^{hf} \right|}{\sum_{i=1}^{I} s_i}. \tag{2.8}$$

The idea relies on the assumption that the frequency portion of the signal indicates high randomness, which is difficult to predict. The customers are subsequently clustered, using clustering algorithms such as K-means, and conventional CBL estimation methods are applied to the clusters. It was shown by the same authors, through simulation, that CBL estimation by DFT clustering yields increased error performance when compared to the standalone conventional CBL estimation methods and other clustering methods.

2.7   Adjustment of CBL estimation methods

Many factors, such as weather and symmetry of a period to the DR event, may affect a household's consumption profile prior to the DR event period [23]. Therefore,

a mechanism can be introduced to adjust the baseline more appropriately to reflect estimated customer usage during the event. Figure 2.1 illustrates the concept of CBL adjustment. The actual consumption decreases relative to the non-event period as a result of the DR notice. However, the decrease in actual consumption, which began at the notice time, is not significant until the start of the DR event. This discrepancy can be adjusted in order to create a sort of "symmetry" in the consumption–baseline relationship in the non-event and event periods. The adjustment is created with the adjusted CBL baseline in the period referred to as the adjustment window, which is usually some hours before the start of the event.

Baseline adjustment is usually computed using historical data of temperature or consumption profile prior to a DR event [24]. In this study, baseline adjustment is estimated with the consumption data. The most common adjustment methods are additive adjustment and multiplicative adjustment. The former employs absolute change between actual consumption and initial baseline to compute the adjusted CBL, while the latter uses the percentage change and applies it to the initial baseline.

Let the pre-event adjustment window be denoted by $\mathcal{P}'$, and each adjustment time slot by t', such that $t' \in \mathcal{P}'$. Additive adjusted CBL can be computed as

$$\mathrm{CBL}_i^{\mathrm{adj}}(d,t) = \mathrm{CBL}_i(d,t) + \frac{\sum_{t' \in \mathcal{P}'} \left(L_i(d,t') - \mathrm{CBL}_i(d,t') \right)}{|\mathcal{P}'|}, \tag{2.9}$$

and the multiplicative adjusted CBL is

$$\mathrm{CBL}_i^{\mathrm{mult}}(d,t) = \mathrm{CBL}_i(d,t) \times \frac{\sum_{t' \in \mathcal{P}'} L_i(d,t')}{\sum_{t' \in \mathcal{P}'} \mathrm{CBL}_i(d,t')}. \tag{2.10}$$
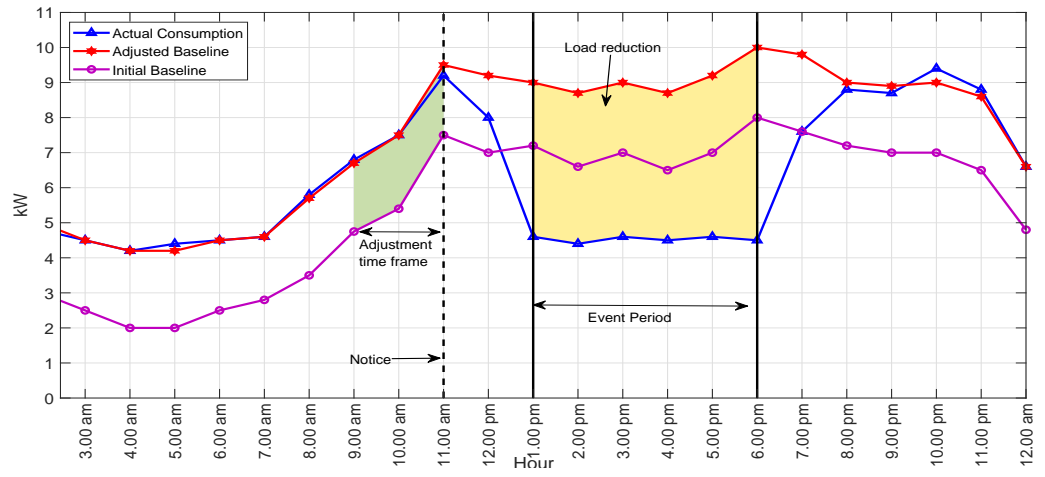
Figure 2.1: Illustration of demand response energy reduction with adjusted and un-adjusted baselines, adapted from [25].

CHAPTER 3: PROPOSED CBL ESTIMATION METHOD

Clustering algorithms rely on similarity and dissimilarity in the feature(s) of signals to group them into unique clusters. In the DFT clustering discussed in Chapter 2, households are grouped based on their Performance Index with similar values in this same cluster. Although the DFT clustering has been shown to provide improved CBL estimation accuracy, in this study, I exploit the advantage of wavelets over DFT to further improve the CBL accuracy. Wavelets represent signals in terms of functions that are localized in both time and frequency, whereas the Fourier transform is only localized in frequency. Thus, transforming signals by DFT loses information about time. In this study, I leverage the advantage of wavelets to extract features from the signals representing the customers' time-series consumption profiles to estimate the CBL via clustering.

Various wavelet-based approaches are employed for feature extraction from a signal depending on the targeted application. The traditional Discrete Wavelet Transform (DWT) decomposes the signal into scaling coefficients. However, the signal representation (coefficients) are too coarse for practical in-depth multi-resolution analysis. Maximal Overlap Discrete Wavelet Transform (MODWT) is a modified version of DWT. In MODWT, the coefficients are "non-decimated," which implies that the number of the original signal sample observations is the same as the number of scaling and wavelet coefficients at every level of the transform [19]. Wavelet Packet Transform (WPT) provides a richer resolution than the DWT. Unlike DWT where only the low frequency coefficients are decomposed to the next level, both low and high frequency coefficients are decomposed in WPT. In this study, I exploit the undecimated form of the wavelet packet decomposition–Maximal Overlap Discrete Wavelet

Packet Transform (MODWPT)–for the feature extraction required for the clustering of the customers.

The application of MODWPT in the estimation of DR event CBL is delineated in Figure 3.1.
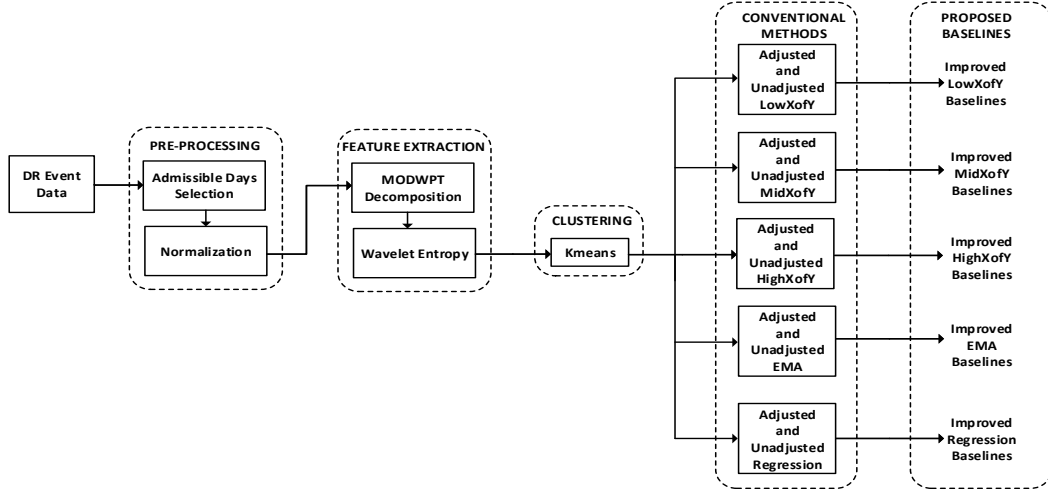
Figure 3.1: Block diagram showing the procedure of the proposed CBL estimation method.

3.1   Overview of Maximal Overlap Discrete Wavelet Packet Transform (MODWPT)

In addition to the relative finer resolution of MODWPT, the motivation of harnessing MODWPT over DWT is the flexibility in the selection of the starting point of the considered time-series signal. For instance, the application of MODWPT is not sensitive to any chosen starting point in the historical profile of a household's consumption data. Figure 3.2 depicts the illustration of decomposition of a time-series signal $\mathbf{S}$.

The MODWPT filters used to decompose signal $\mathbf{S}$, whose dimension N is indexed by $t = 0, 1, \cdots, N - 1$, can be expressed in terms of the discrete WPT quadrature mirror filters: the wavelet filter g_l and the scaling filter h_l. The filters are equivalent to high pass and low pass filters, and are used to compute the approximation and

detail coefficients, respectively. Let the decomposition level of MODWPT be indexed by $j = 0, 1, \cdots, J$. Furthermore, the node (equivalent to frequency index) of jth level of the decomposition tree is indexed by $n = 0, 1, \cdots, 2^j - 1$. The jth level coefficient vector of the MODWPT is denoted by $\widetilde{\mathbf{Z}}_{j,n}$, whose decomposed frequency into 2^j equal widths is in interval $[0, f_s/2]$. f_s is the sampling frequency. Thus, the nth node in the jth level is associated with frequency interval $\frac{f_s}{2^{j+1}} [n, n+1]$.
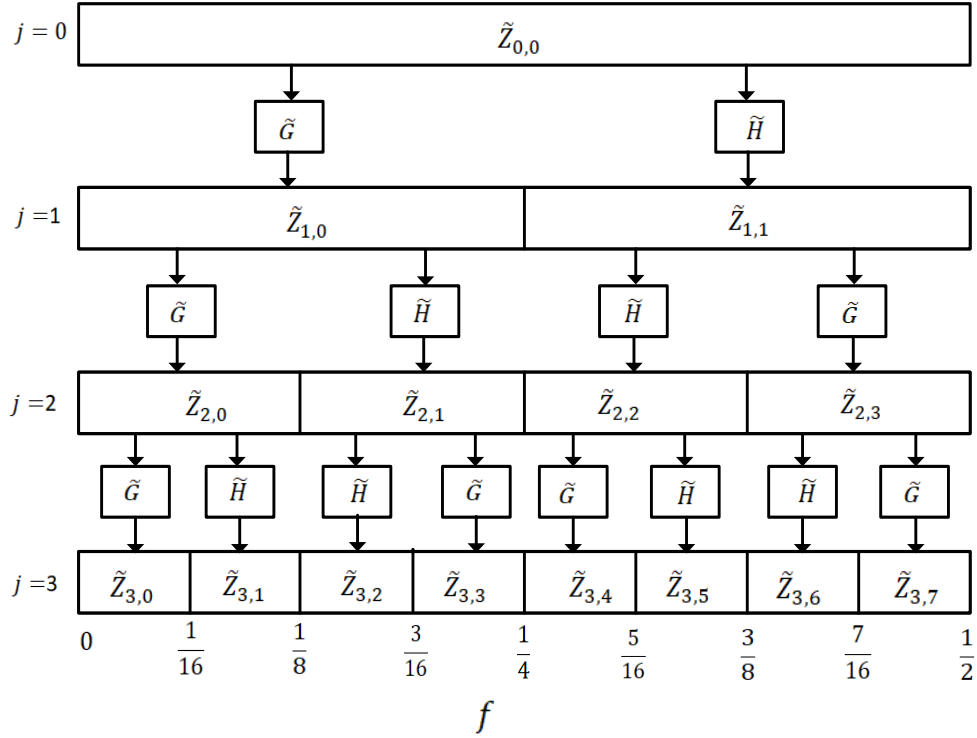
Figure 3.2: Illustration of wavelet decomposition of a time domain signal $\widetilde{\mathbf{Z}}_{0,0} = \mathbf{S}$ into MODWPT coefficients $\widetilde{\mathbf{Z}}_{j,n}$ of levels $j=1$, 2 and 3. In terms of frequency, MODWPT transforms time domain signal $\mathbf{S}$ into frequency bands and central frequencies called nodes. For example, wavelet coefficients in $\widetilde{\mathbf{Z}}_{3,5}$ represent the frequency content in $\mathbf{S}$ for frequencies f such that $|f| \in \left[\frac{5}{16}, \frac{3}{8}\right]$.

For illustration, the MODWPT decomposition tree for $J = 3$ presented in Figure

3.2. shows the associated frequencies (as a function of sampling frequency) at the 3rd level.

The tth element coefficient of $\widetilde{\mathbf{Z}}_{j,n}$ is obtained from the filtering of the original time-series $\mathbf{S}$ as [19]

$$\widetilde{Z}_{j,n,t} = \sum_{l=0}^{L_j-1} \widetilde{v}_{j,n,l} S_{j-l \bmod N}, \ t = 0, \cdots, N - 1, \tag{3.1}$$

where $\widetilde{v}_{j,n,l}$ is a composite filter $v_{j,n,l}$ derived from DWPT filter as

$$\widetilde{v}_{j,n,l} = \frac{v_{j,n,l}}{2^{j/2}}. \tag{3.2}$$

The $v_{j,n,l}$ filter is realized as

$$v_{j,n,l} = \sum_{k=0}^{L-1} v_{n,k} v_{j-1,\left\lfloor \frac{n}{2} \right\rfloor, l-2^{j-1}k}, \ l = 0, \cdots, L_j - 1, \tag{3.3}$$

where $L_j = (2^j - 1)(L - 1) + 1$, and

$$v_{n,l} = \begin{cases} g_l, & \text{if } n \bmod 4 = 0 \text{ or } 3 \\ \\ h_l, & \text{if } n \bmod 4 = 1 \text{ or } 2, \end{cases} \tag{3.4}$$

and $v_{1,0,l} = g_l$ and $v_{1,1,l} = h_l$. The scaling filter g_l is the quadrature mirror of the wavelet filter h_l, that is, $g_l = (-1)^{l+1} h_{L-1-l}$.

The details at the nth node of the jth level MODWPT is depicted by $\widetilde{\mathcal{D}}_{j,n}$, whose tth element is derived as

$$\widetilde{\mathcal{D}}_{j,n,t} = \sum_{l=0}^{L_j-1} \widetilde{v}_{j,n,l} \widetilde{Z}_{j,n,t+l \bmod N}. \tag{3.5}$$

Thus, the original time-series signal can be reconstructed in terms of the details as

$$S_t = \sum_{n=0}^{2^j-1} \widetilde{\mathcal{D}}_{j,n,t}. \tag{3.6}$$

3.2 Feature Extraction from MODWPT Coefficients

As it has been shown so far in this section, the output of the MODWPT decomposition is a vector of coefficients that cannot directly be used as clustering features. The coefficients are reduced to feasible high-level features: energy and entropy. The features in the MODWPT detail coefficients exactly align with the features in the original signal. As stated in Eq. (3.6), summing up the MODWPT details for each sample, at a specified level, gives the exact original signal. Similarly, the MODWPT coefficients energies are equal to the sum of the energy in the original signal. Since the energy of the original signal is preserved in the MODWPT coefficients energies, I compute entropy from the energies and use the calculated entropy as the original signal's representative features.

Signal **S** is a vector made up of stacked observations from a single household consumption over the days under consideration. The energy of MODWPT coefficient of each node at the jth level for a signal vector **S** is computed as

$$E_{j,n,t} = \left| \widetilde{Z}_{j,n,t} \right|^2. \tag{3.7}$$

where t refers to each point (coefficient), n the node, and j the level. And the total energy of all the points in a node is obtained as

$$E_{j,n} = \sum_{t=1}^{N} E_{j,n,t}, \tag{3.8}$$

where N is the number of the corresponding coefficients in the node.

The probability value of the tth coefficient at its corresponding node can be calculated via normalization as

$$P_{j,n,t} = \frac{E_{j,n,t}}{E_{j,n}}. \tag{3.9}$$

$P_{j,n,t}$, also known as *relative wavelet energy*, denotes the probability distribution of energy and $\sum_n P_{j,n,t} = 1$.

Shannon information entropy has been prevalently used in information theory, signal processing, artificial intelligence, genomics, etc. However, the combination of wavelet analysis with entropy is more effective than pure information entropy in the signal analysis of power systems. The combination provides a rich representation of features information due to the full use of localization ability of wavelets in both time and frequency domain [26]. When used to analyze a power signal, the wavelet entropy statistically reflects the distribution of the important energy information in the signal. The identification of the important features is otherwise referred to as *feature extraction*. The goal of feature extraction is to transform the original feature-space of a signal into a new space that represents the important characteristics that are otherwise not directly observable in the original space. The wavelet entropy feature is expressed in terms of relative wavelet energy via Shannon entropy formula as

$$WE_{j,n} = -\sum_n P_{j,n,t} \cdot \log(P_{j,n,t}), \tag{3.10}$$

which depicts the value of wavelet energy entropy at each node. Since there are 2^J number of nodes in a J-level MODWPT, $WE_{j,n}$ can be alternatively denoted as WE_p, for clarity, to form the stack of $P = 2^J$ energy entropy of a signal as

$$\boldsymbol{W} = [WE_1, \cdots, WE_P], \tag{3.11}$$

where the dimension of $\boldsymbol{W}$ is $1 \times P$. For instance, dimension of $\boldsymbol{W}$ would be 1×16 with a four-level MODWPT.

3.3   Household Clustering

Clustering implies the organizing of unlabeled data into similarity groups (called clusters) based on some feature(s). Since the data to be grouped is unlabeled, clustering techniques are regarded as unsupervised learning algorithms. K-means [27, 28], a widely-known and efficient partitioning clustering technique, is used to form a small number of clusters from a large number of observations. As each household consumption is represented by its corresponding wavelet entropy, K-means is employed to group the households, with respect to the entropy observations.

Suppose for the household set participating in a DR event is represented by the set $\mathcal{I} = \{1, \cdots, I\}$ and each household wavelet entropy described as $\boldsymbol{W}_i \in \mathcal{W}$, the goal of K-means is to find K centroids and the corresponding label for each observation (household). The algorithm starts initializing some random numbers of cluster centroids $\mu_1, \cdots, \mu_K$. The resulting procedure aims at minimizing the total intra-cluster variance:

$$\sum_{k=1}^{K} \sum_{h=1}^{H} \|\boldsymbol{W}_i - \mu_k\|^2 , \qquad (3.12)$$

where $\|\boldsymbol{W}_i - \mu_k\|^2$ is the Euclidean distance function iterated overall h observations in the jth cluster and for all K clusters. Calinski-Harabasz.

The changes in the cluster distribution after several runs of clustering (Kmeans) algorithm is evaluated by clustering robustness. The smaller the change after many repeated runs of a clustering algorithm, the more robust the clustering. The clustering robustness can be used to obtain the appropriate number of clusters to group the data observations. In the survey and evaluation of methods for choosing the number of clusters in [29], the Calinski-Harabasz [30] is found to be the most robust. Thus,

in this work, the number of clusters is determined using Calinski-Harabasz method. The clustering robustness by Calinski-Harabasz method is obtained as [31]

$$CR\left(k\right) = \frac{\sum_i^k n_i d^2\left(c_i, c\right)/\left(k-1\right)}{\sum_i^k \sum_x c_i d^2\left(x, c\right)/\left(n-k\right)}, \tag{3.13}$$

where n is the number of observations, K the number of clusters, C_i the $i$the cluster, n_i the number of observations in C_i, c_i the center of C_i, x is a point in cluster C_i, and $d\left(\cdot\right)$ is the Euclidean distance between two points. From any K set of clusters evaluated, the optimal number of clusters can be obtained by maximizing the function $CR\left(k\right)$.

$$k^{\text{opt}} = \arg\max_k CR\left(k\right). \tag{3.14}$$

CHAPTER 4: CASE STUDY DR PROGRAM

The trial demand response (DR) program was part of the Smart Grid, Smart City (SGSC) customer applications program [10]. The SGSC was an Australian government's energy efficiency initiative targeted to deliver a commercial-scale DR program over smart grid infrastructures.

The Ausgrid consortium was selected as the program tenderer by the Australian government. Ausgrid is an electricity distribution company that maintains and operates electric grids in New South Wales, Australia. EnergyAustralia was the collaborating partner of Ausgrid in the demand response program. EnergyAustralia is an electricity retailing company in Australia. In the DR program, Ausgrid served as the distribution network service provider (DNSP), and EnergyAustralia was the electricity retailer. The DR events were conducted from 2010 to 2014, but the available DR data in [32] spanned from 2013 to 2014.

The program was focused on greater Newcastle and Sydney CBD areas, in addition to four additional zones (Ku-Ring-Gai, Newington, Scone, Nelson Bay areas). Thus, the covered areas are a mix of both urban and rural areas, but captured customers are all residential. The deployment of smart meter infrastructure with meter management systems and back-office systems facilitated the SGSC implementation. Smart meters were allocated for Customer Applications, Grid Applications, Distributed Generation and Storage, and Electric Vehicle trials. The scope of this study is confined within Customer Applications since our interest is on CBL.

The events records provided in [32] consists of a total of 28 events. Events were designed to last between one and four hours and were only to be called between 2 pm and 8 pm on working weekdays.

4.1 Enabling Technologies

Some devices were employed for household electricity consumption usage and monitoring customer behaviors. For usage measurement, 17,134 smart meters were deployed for the Customer Applications trial [10].

Also utilized were feedback technologies. These are devices or platforms used to measure the behavioral changes of electricity customers based on their use [10]. The technologies are in-home display (IHD), an online portal, and smart plugs.

IHD is a small portable device used to inform customers of price changes or DR events. The device displays electricity usage and real-time pricing information. The IHD's display comprises of a simple interface where the metering, price, and message data are presented. The IHD employed in the SGSC program is shown in Figure 4.1.
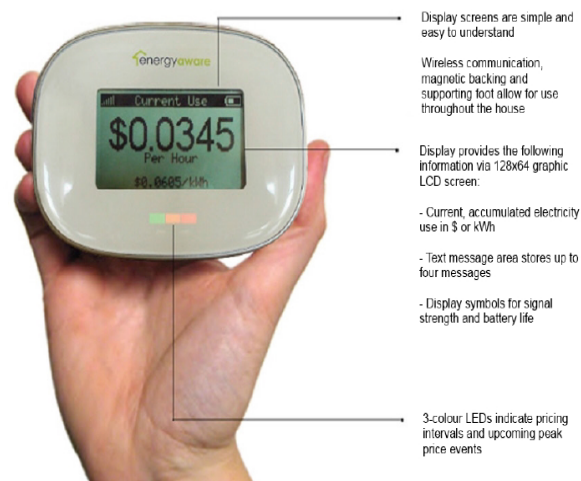
Figure 4.1: In-home display device [10].

The online portal is an online electricity usage management website designed to provide information about household meter data in almost real-time. The portal is accessible from a computer, tablet, and smartphone. Figure 4.2 displays an example of the online portal interface designed for the DR program.

Figure 4.2: Online portal [11].

Smart plugs are devices used to sub-meter and control multiple appliances connected to the general power outlet. The appliances can be controlled (switched on or off) via the setup online portal or a mobile device. The smart plug computed the electricity consumption of the appliances and wirelessly transmit the periodic total usage to the smart meter. Figure 4.3 shows the Jetlun smart plug used in the SGSC program.

Customers in the trials were randomly assigned to one of no feedback technology, one feedback technology, or two feedback technologies. Since the focus of this paper is on CBL estimation, the analysis of customer behavioral changes will be studied in future works.

Figure 4.3: Jetlun smart plug [11].

4.2   Pricing Structures

Two peak event pricing plans were used to incentivize customers to reduce their electricity consumption during specified peak events. Before the introduction of the DR programs, participating customers were on one of the two pricing structures: All-Time and Time-of-Use (ToU). Customers on the All-Time plan paid a flat rate all day, every day. Conversely, the ToU plan has varied rates based on the time of the day. The two pre-DR pricing plans are illustrated in Figure 4.4.

During the DR events, the pricing plans could be largely grouped into three categories: the existing (pre-DR) plan, Dynamic Peak Price (DPP) tariff, and Dynamic Peak Rebate (DPR) tariff. For evaluation of DR program, only the DPP and DPR are relevant.

Once the DPP DR program started, the participants' consumption on the DPP event days resumed a time-varying tariff. The tariff is shown in Figure 4.5. Consumption is billed 13.09 cents/kWh from 12am to 7am and 10pm to 12am. 24.53 cents/kWh is the rate between 7am and 10pm, except for the peak period that the

tariff spikes to 330.00 cents/kWh. Ten peak events with DPR were conducted as recorded in [32]: 3 in Summer 2013, 1 in Autumn 2013, 2 in Spring 2013, and 4 in Summer 2014. Although DPP event dates are listed in the information publicly made available in [10], the DPP DR response consumption and payment information are not included in the DR response data. Therefore, I focus on the evaluation of DR with respect to DPR in this study.
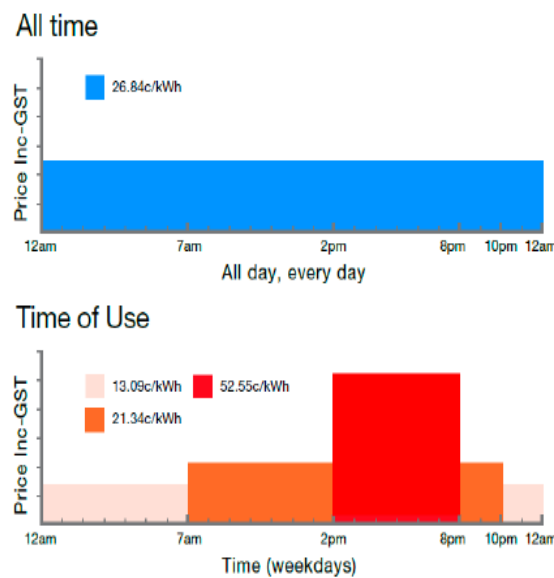
Figure 4.4: All-Time (top) and Time-of-Use (bottom) pre-DR pricing plans [11].

DPR is the other tariff plan offered to the DR program participants. 18 DPR peak events were conducted as recorded in [32]: 4 in Summer 2013, 4 in Autumn 2013, 5 in Winter 2013, 2 in Spring 2013, and 3 in Summer 2014. In DPR, the participants received a rebate based on their reduction in electricity consumption during the DR events. However, the exact rebate computation formula was neither revealed to the customers nor in the reports [11]. In order to evaluate the DR programs with respect to the rebate paid, I estimate the rebate payment using clustered linear regression.
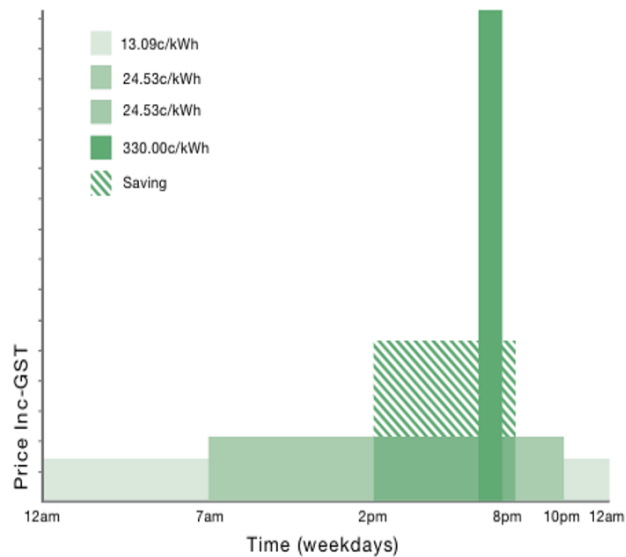
Figure 4.5: Dynamic peak pricing [11]. The shaded stripes area shows the peak period (2pm to 8pm) savings from DPP plan relative to ToU plan.

4.3   Datasets

The proposed CBL estimation method and Dynamic Peak Rebate (DPR) pricing were analyzed using the data from actual DPR demand response events. The data subsets for the selected events were extracted from the data files made publicly available by the Australia Government in [32]. The list of the 28 DR events and their corresponding pricing structure was posted. In addition, the data source website includes the data for the actual household consumption during the DR period, the baseline consumption, and the paid rebates for the participants in DPR events.

The data source includes the Electricity Use Interval Reading file, which is a time-series data of households' electricity usage in 30-minute intervals from 2012 to 2014. Since there was no uniform sign-up date, the interval consumption record is not consistent across households. Based on the DPR events and the participant IDs, corresponding customer's consumption interval data were extracted.

4.4   Selection of the Case Study DR Events

The fifth column of Table 4.1 shows the number of participants whose data are captured in the DR response data file made available in [32]. Although the participants in the DPR demand response programs are residential customers, the covered regions are a mixture of both urban and rural areas.

To avoid the risk of working with data that are very unrepresentative of the population, I decided to use DR events where participants are at least a thousand. The rationale is that a larger sample size will reduce the imbalance of customer representation in favor of either rural or urban households. In event 1000261, the participants inexplicably got rebates for exceeding baselines. Standard methods cannot deduce rebates paid in event 1000265. Therefore, events 1000261 and 1000265 are excepted from the events evaluated in this work despite each having at least a thousand participants. The DPR events used as case study events are labeled Event I to Event III and written in bold letters in Table 4.1.

Table 4.1: DR events with dynamic peak rebate (DPR) pricing structure including the 3 selected events for this research

Event ID	Event Day	Season	Start Time	End Time	Number of Customers	Event Label§
1000240	2013-01-17	Summer	12:00	16:00	150	
1000241	2013-01-25	Summer	13:00	17:00	217	
1000242	2013-02-08	Summer	13:30	17:30	789	
1000244	**2013-03-07**	Autumn	**11:30**	**15:30**	**1042**	**I**
1000245	2013-03-13	Autumn	13:00	17:00	1135	
1000246	2013-03-22	Autumn	13:30	17:30	1185	
1000248	**2013-03-28**	Autumn	**11:30**	**15:30**	**1169**	**II**
1000249	2013-06-25	Winter	16:00	18:00	0	
1000250	2013-07-24	Winter	16:30	19:30	1159	
1000251	**2013-08-02**	Winter	**16:30**	**19:30**	**1153**	**III**
1000252	2013-08-08	Winter	16:30	20:00	0	
1000253	2013-08-22	Winter	17:00	20:00	0	
1000254	2013-09-26	Spring	15:00	18:30	0	
1000256	2013-11-28	Spring	14:00	18:00	0	
1000258†	2013-12-04	Summer	13:00	17:00	981	
1000261†	2014-01-16	Summer	13:00	17:00	1000	
1000265‡	2014-01-31	Summer	13:00	17:00	1023	
1000266	2014-02-13	Summer	13:00	17:00	1021	

* Number of participants with data in the DR response file in the data source [32].
§ The descriptive names used for the selected events analyzed in this research.
† Participants inexplicably got rebate for exceeding baseline.
‡ Rebate cannot be deduced by standard methods.

CHAPTER 5: ESTIMATION WITH CLUSTERED LINEAR REGRESSION

The amount of rebate paid in the case study DR program is informed by the load reduction (the difference between the CBL and the actual load) at the event period. The data exploratory (plots and inspection) of the rebate amount with respect to the load reduction shows the partition patterns.

In the rebates paid in selected case study DR events I, II and III, two clusters are observed: a group of customers with negative load reduction that received zero rebates, and the other group are the customers with positive load reduction with rebate paid as a function of the consumption reduction. To deduce the rebate pricing from the available paid rebate data for the events mentioned above, I employed clustered linear regression (CLR) Model.

CLR model is a linear regression model in which the homoscedasticity assumption is relaxed. That is, the model allows the error terms to be heteroscedastic and correlated within groups. With CLR, linear approximation on multiple subspaces can be performed. The procedures to implement CLR include finding the number of the clusters, determining the boundaries of the clusters, and performing individual regression on observations within each cluster [33]. I employed the *split-apply-combine strategy* [34] to implement the CLR procedures in this work. Figure 5.1 illustrates the application of the strategy to CLR.
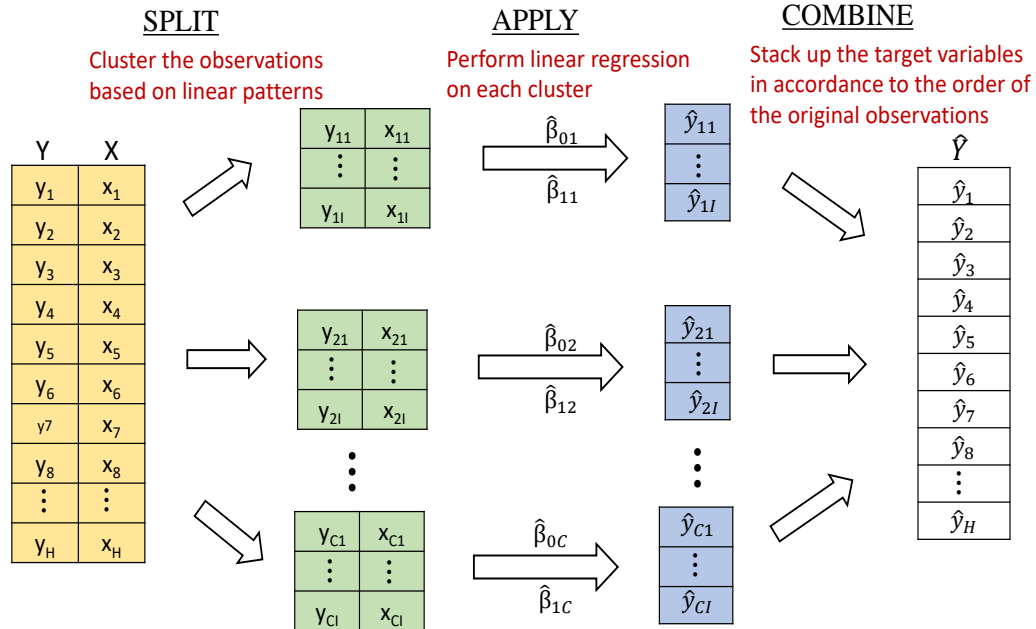
Figure 5.1: Application of Split-Apply-Combine strategy to clustered linear regression.

5.1   Split-Apply-Combine Strategy

It is noteworthy that the CLR via the split-apply-combine strategy in this work implies training the data. I trained the rebate dataset (with rebate amount and load reduction as the dependent and independent variables, respectively) to obtain the estimates of the intercept and slope for each cluster. The obtained regression coefficients were used to estimate the rebate amount paid for the three DR events. The split phase involves grouping of the data feature(s) based on some criteria. Regression is performed on the individual group (cluster) in the apply phase. Lastly, the obtained regression results (predictors) from the clusters are combined.

Based on a simple linear regression model

$$Y = \beta_0 + \beta_1 X + \epsilon, \tag{5.1}$$

where β_0 and β_1 are two unknown coefficients depicting the intercept and slope, the rebate amount from each observation (household) can be described as

$$y_{ci} = \beta_{0c} + \beta_{ci} x_{ci} + \epsilon_{ci}, \quad i \in \mathcal{I} \tag{5.2}$$

where observations in cluster $c = 1, \cdots, C$ are indexed by $i = 1, \cdots, I$. Since the energy consumption in each household is mutually independent, $\epsilon_{ci} \sim \mathcal{N}(0, \sigma_{ci}^2)$. The rebate amount estimate is the dependent variable y_{ci}, and load reduction of each observation is denoted by x_{ci}. In the case study DR events I, II, and III, x_{c1} is a positive load reduction (baseline higher than the actual consumption), and x_{c2} is a negative load reduction (baseline less than the actual consumption). The paid rebates for each y_{c1} and y_{c2} were available. Thus, the coefficients can be estimated. Since there could be different numbers of observations per cluster, I denote the total observation particular to a cluster as I_c. Thus, $H = \sum_{c \in C} I_c$ represents the total number of households (observations) participating in a DR event.

In the split phase, the criteria are typically user-defined based on values of the observations. From the observed data patterns, I define the splitting criteria for rebate amount y_i based on load reduction x_i in the case study DR events I, II, and III as

$$y_i = \begin{cases} y_{1i}, & \text{if } x_i >= 0 \\ y_{2i}, & \text{otherwise.} \end{cases} \tag{5.3}$$

The above criteria reflect zero rebate payment for negative load reduction (i.e., when actual load during the event period is greater than the CBL). In the regression equations, x_i is described as x_{ci} to indicate the cluster it is associated with after applying the splitting criteria. Stacking the observations within a cluster, the model at the cluster level can be written as

$$Y_c = \beta_{0c} + \beta_{1c} X_c + \epsilon_c, \tag{5.4}$$

where Y_c, X_c and ϵ_c are each $I_c \times 1$ vector, and $\epsilon_c \sim \mathcal{N}\left(0, \sigma_c^2\right)$.

In the apply phase, linear regression is performed on each individual cluster, according to Eq. (5.2), to obtain the the estimates $\hat{\beta}_{0c}$ and $\hat{\beta}_{1c}$. The coefficient estimates were used to compute the rebate estimate for each cluster, $\hat{Y}_c = \hat{\beta}_{0c} + \hat{\beta}_{1c} X_c$. For a straight line cluster, the equation of the line is used instead performing linear regression

Finally in the apply phase, cluster-level rebate estimates are stacked to form the rebate estimate for an event. That is, $\hat{Y} = [\hat{y}_1, \cdots, \hat{y}_C]^\top$, which is a $H \times 1$ vector. $\hat{Y}$ is subsequently sorted according to the order of the original observations. That is, $\hat{Y} = [\hat{y}_1, \cdots, \hat{y}_H]^\top$. The accuracy of $\hat{Y}$ for each event is validated with R-squared.

5.2   Results of Rebate Payment Estimation

Figures 5.2 - 5.4 show the original rebates (observations) and the regression lines obtained by CLR. Moreover, the results of the cluster regression coefficients for each of the three events are presented in Table 5.1.

Table 5.1: The regression coefficients and R-squared of the rebate estimate determined by CLR model

| Events | Clusters | Regression Coefficients | | R-squared |
		Intercept ($\hat{\beta}_{0c}$)	Slope ($\hat{\beta}_{1c}$)	
I	1	0.0470	4.4944	1.0000
	2	0	0	
II	1	0.0897	4.899	0.9999
	2	0	0	
III	1	0.0323	4.4953	1.0000
	2	0	0	
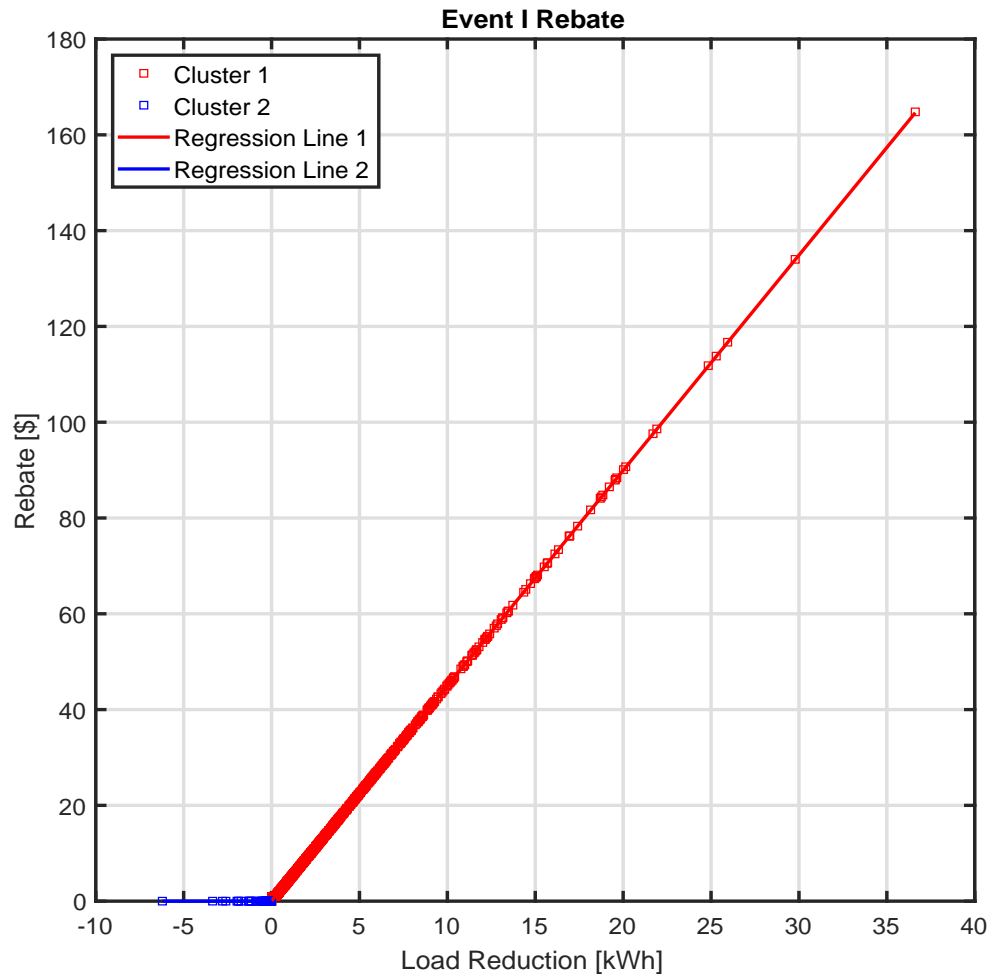
Figure 5.2: Event I rebate estimation with clustered linear regression.
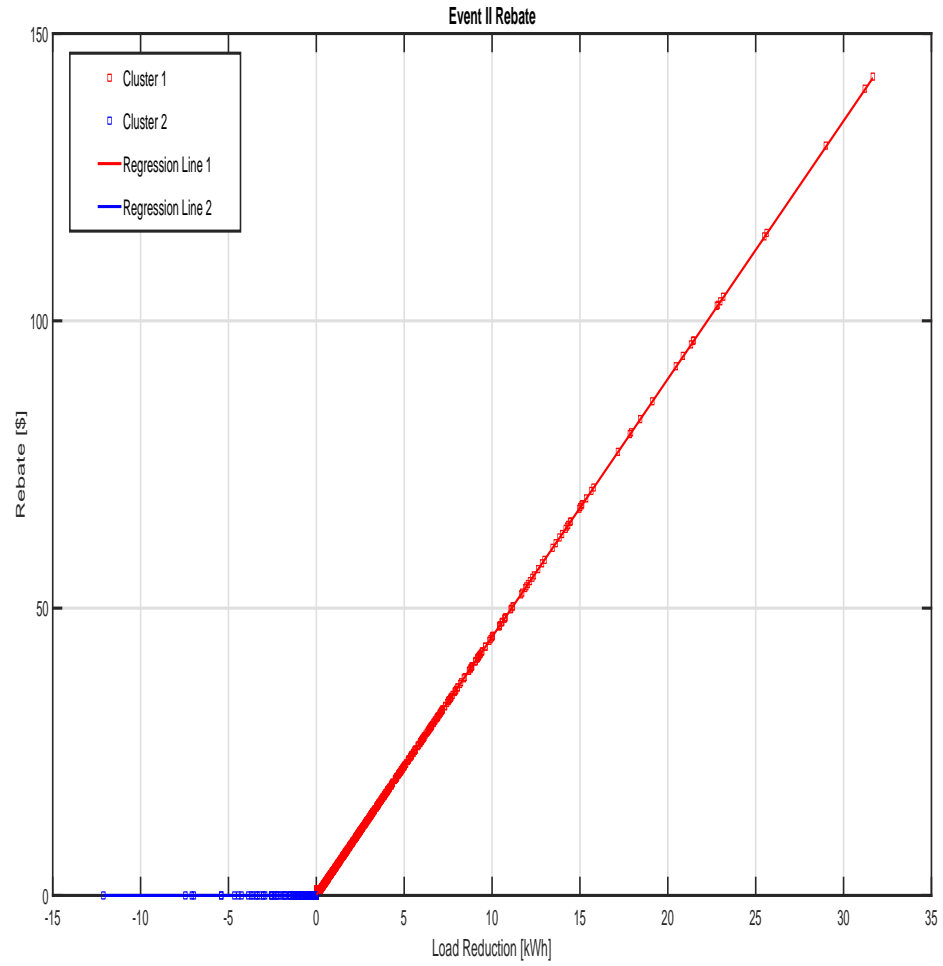
Figure 5.3: Event II rebate estimation with clustered linear regression.
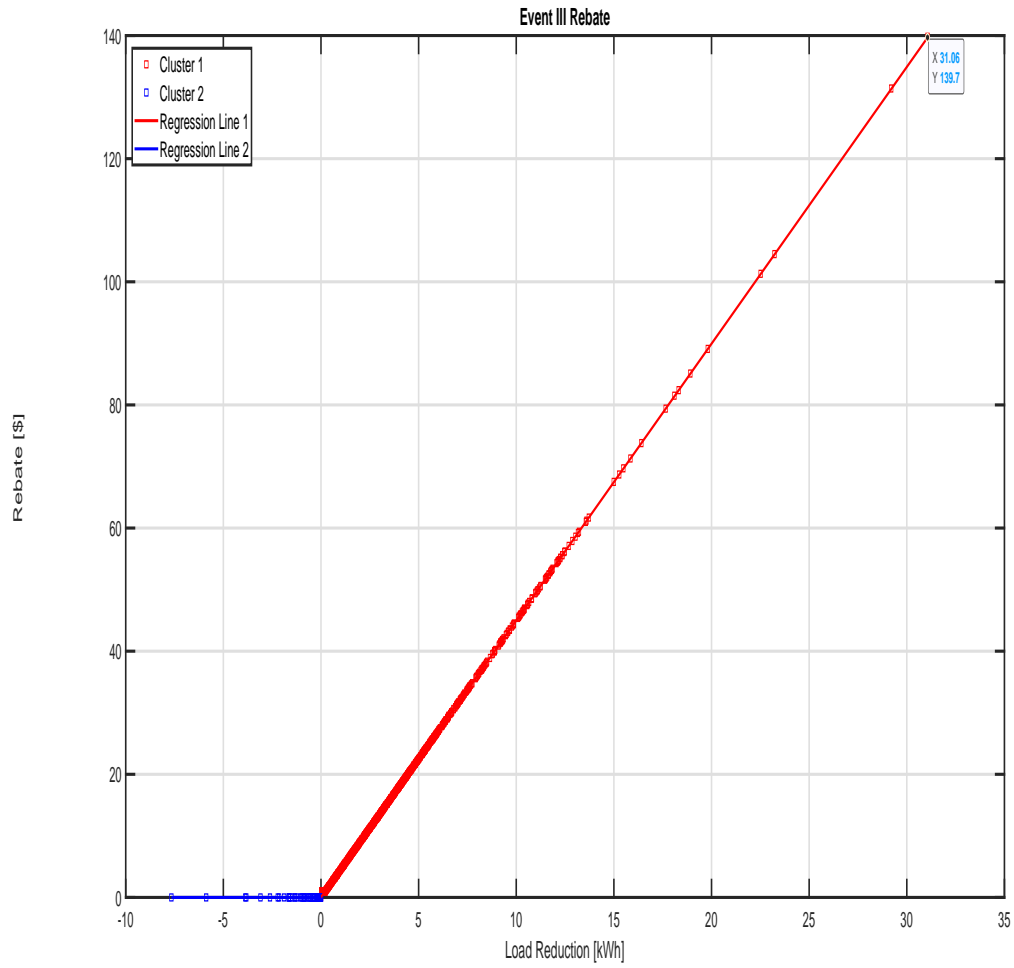
Figure 5.4: Event III rebate estimation with clustered linear regression.

CHAPTER 6: IMPLEMENTATION, RESULTS AND DISCUSSIONS

In this chapter, the implementation of the proposed CBL estimation method is discussed. The performance evaluation of the method, compared to the benchmark methods and the DFT clustering technique, is also presented. Furthermore, I analyze the performance of Dynamic Rebate Pricing using the selected three DR events with respect to the proposed and benchmark CBL methods.

6.1   Counterfactual DR Consumption and Incentive Payment

In practice, the DR event would affect the consumption of a given customer. Since DR participants are pre-notified of a DPR event, customers are likely to adjust their consumption to receive rebates. Thus, the direct prediction of event day consumption will not be as accurate as possible. One way to approach such a problem is to compare different groups in a randomized controlled trial (RCT).

To obtain a true estimate of event day consumption will require a randomized selection of control (non-DR participants) and treatment (DR participants) groups. Although the case study DR program considered in this work includes the use of a control group, the selection of customers into the group is not statistically random [10, 35]. Another approach is the load impact computation [36, 20], which estimates the *counterfactual* consumption. The counterfactual consumption is the consumption during the peak period in the hypothetical absence of a DR event. The load impact is determined from the estimate of baseline on real DR event day d, and used for estimating the counterfactual consumption $\hat{L}_i(d', t)$ on a proxy event day d'. I follow the approach of [20] of estimating counterfactual consumption of a proxy event with

the load impact from a target DR event. The load impact is obtained as

$$impact = \frac{\sum_{i \in \mathcal{I}} \sum_{t \in \mathcal{P}} (\text{CBL}_i(d,t) - L_i(d,t))}{\sum_{i \in \mathcal{I}} \sum_{t \in \mathcal{P}} \text{CBL}_i(d,t)}. \tag{6.1}$$

The load impact approach to baseline evaluation relies on the assumption that the impact obtained from known data of an actual DR event can be assumed to be the demand reduction rate of same DR participants on a hypothetical DR event day having the same rebate pricing structure and similar weather conditions. The counterfactual consumption can be estimated as a given proxy day consumption after adjusting for the load impact. Therefore, counterfactual consumption for a given proxy day can be computed as

$$\hat{L}_i(d',t) = (1 - impact) \cdot L_i(d',t), \tag{6.2}$$

where $L_i(d',t)$ is the actual consumption of customer i on the proxy day during the peak period timeslot $t \in \mathcal{P}$.

To achieve close similarity between the proxy and the target event days in terms of load demand and weather conditions, I ensured the following. I chose a proxy day in the same month as the target DR event day. The candidate proxy day is a weekday, non-holiday, and a non-DR day. Since there are some months with multiple events, the candidate proxy day with the highest daily consumption after the previous DR event is selected as the proxy of the target future DR event. After applying the stated criteria, the selected proxy days for the three chosen events are one day before the target DR event days. Table 6.1 gives summary information about the selected DR events and their corresponding proxy days.

The incentive payment evaluation via the load impact approach also requires that the same payment rule and rebate pricing structure applied to the target DR event

Table 6.1: Description of the selected case study DR events and corresponding proxy days

Label	DR Event	Date	Season	Duration (hours)	Start Time	End Time
I	**Actual**	**2013-03-07**	Fall	4	11:30	15:30
	Proxy	2013-03-06				
II	**Actual**	**2013-03-28**	Fall	4	11:30	15:30
	Proxy	2013-03-27				
III	**Actual**	**2013-08-02**	Winter	3	16:30	19:30
	Proxy	2013-08-01				

load reduction is equally applied to the counterfactual consumption reduction [36, 20]. According to the case study DR program payment rule, customers with a negative load reduction receive no incentive. Customers with positive load reduction receive an incentive according to the amount of reduced load. However, the rebate rate was not revealed by the Australian DR operator. Since data on event period consumption, baseline, and rebate payment was available, I estimated the paid rebate rate for the target DR events using clustered linear regression discussed in chapter 5. The coefficients β_0 and β_1 for the regression of the actual rebate R_i^{act} paid for load reduction $\sum_{t \in \mathcal{P}} \left(\mathrm{CBL}_i(d, t) - L_i(d, t) \right)$ on a target event day d is obtained using the linear regression equation

$$R_i^{\mathrm{act}} = \beta_0 + \beta_1 \sum_{t \in \mathcal{P}} \left(\mathrm{CBL}_i(d, t) - L_i(d, t) \right). \tag{6.3}$$

With the obtained coefficients, the same rebate rate applied to the target DR load reduction can be applied to that of the proxy event for the evaluation of incentive payment. The ideal rebate for the load reduction on a proxy day d' with customer i estimated counterfactual consumption $\hat{L}_i(d', t)$ can be calculated as

$$R_i = \beta_0 + \beta_1 \sum_{t \in \mathcal{P}} \left(L_i(d', t) - \hat{L}_i(d', t) \right), \tag{6.4}$$

where $L_i(d', t)$ is the actual consumption of customer i on the proxy day during the peak period timeslot $t \in \mathcal{P}$. Let the load reduction on the proxy day d' estimated by a given baseline be depicted by $\sum_{t \in \mathcal{P}} \left(\text{CBL}_i(d', t) - \hat{L}_i(d', t) \right)$. Therefore, the rebate payment estimate based on a given baseline is

$$\hat{R}_i = \beta_0 + \beta_1 \sum_{t \in \mathcal{P}} \left(\text{CBL}_i(d', t) - \hat{L}_i(d', t) \right). \tag{6.5}$$

Following the payment rule of the case study program of paying no rebate to the customers whose actual DR event period consumption is higher than the baseline, I apply the same rule to the proxy event as

$$\hat{R}_i = \begin{cases} \beta_0 + \beta_1 \sum_{t \in \mathcal{P}} \left(\text{CBL}_i(d', t) - \hat{L}_i(d', t) \right), & \text{if } \sum_{t \in \mathcal{P}} \left(\text{CBL}_i(d', t) - \hat{L}_i(d', t) \right) >= 0 \\ 0, & \text{otherwise.} \end{cases} \tag{6.6}$$

Similarly, the ideal rebate stated in Eq. (6.4) can also be expressed in terms of the payment rule as

$$R_i = \begin{cases} \beta_0 + \beta_1 \sum_{t \in \mathcal{P}} \left(L_i(d', t) - \hat{L}_i(d', t) \right), & \text{if } \sum_{t \in \mathcal{P}} \left(L_i(d', t) - \hat{L}_i(d', t) \right) >= 0 \\ 0, & \text{otherwise.} \end{cases} \tag{6.7}$$

6.2   CBL Performance Evaluation Metrics

As explained in section 6.1, DR participants are likely to reduce electricity usage on the actual event day to receive incentives. The demand reduction makes it impossible to evaluate the CBL methods if used to predict the actual DR event day consumption. However, CBL evaluation using proxy event day provides a reliable way of validating a CBL method since the aforementioned causal effect is zero. Customers received no notice of any incentive program on a given proxy day. The advantage of using the proxy day is that impact of demand reduction for an incentive, that can influence the

evaluation of the CBL method prediction accuracy, is eliminated. I follow the metrics used in [37] to evaluate the error performance of the proposed CBL estimation in comparison to the benchmarks using a proxy day approach.

6.2.1   Mean Error

Mean Error (ME) is a measure of estimation bias. It is the mean of the difference between the estimated CBL and the actual consumption on a proxy day d', which is averaged by the number of participating households and all the event hours. The ME is computed as follows.

$$ME = \frac{\sum_{i \in \mathcal{I}} \sum_{t \in \mathcal{P}} \left(\text{CBL}_i(d', t) - L_i(d', t) \right)}{|\mathcal{I}| \cdot |\mathcal{P}|}, \tag{6.8}$$

where $\mathcal{I}$ is the set of households participating in a DR event over period $\mathcal{P}$. The summed difference of the proxy day actual consumption $L_i(d', t)$ from the computed CBL, averaged over $|\mathcal{I}|$ and $|\mathcal{P}|$ reflects the program-level bias of the CBL estimation method. Bias (or ME) can be positive or negative, but, the closer to zero the better. An ME of zero indicates a perfect CBL estimation for a proxy event day, which implies positive and negative errors cancel.

6.2.2   Mean Absolute Error

The mean absolute error (MAE) is a measure of the accuracy of the CBL estimation method. MAE is also computed from the CBL estimation for a proxy event day. MAE is the absolute value of the ME averaged over the number of households participating in a DR program.

$$MAE = \frac{\sum_{i \in \mathcal{I}} \left| \sum_{t \in \mathcal{P}} \left(\text{CBL}_i(d', t) - L_i(d', t) \right) \right|}{|\mathcal{I}| \cdot |\mathcal{P}|}. \tag{6.9}$$

MAE is a *negatively-oriented* score, which means lower values are better. An ideal score is zero for a proxy day baseline prediction.

6.2.3   Overall Performance Index

Bias and accuracy measured by ME and MAE, respectively, are the main metrics for evaluating the performance of a CBL estimation method. Overall Performance Index (OPI), which is the weighted sum of accuracy and bias, provides a single-metric overall evaluation of the estimation method.

$$OPI = \gamma \left| MAE \right| + (1 - \gamma) \left| ME \right|. \tag{6.10}$$

The OPI allows for setting the weight of importance depending on what metric matters more to the DR operator. In this thesis, I select the weight of $\gamma = 0.5$ to apportion equal weight to ME and MAE. A lower OPI is preferable. It implies the CBL is capable of measuring the DR participants' response to the offered rebates [7].

6.3   Rebate Payment Evaluation

6.3.1   Payment Error

The customers in the case study DR program were paid rebates according to their DR load reduction. In the selected DR events, customers are paid only if they reduced their consumption. Customers who exceed the baseline consumption received no rebate.[1] The amount of rebate paid is also dependent on the CBL method used to estimate the baseline [36]. Therefore, an erroneous baseline will result in a wrong rebate estimation. In the evaluation of payment error, the counterfactual demand $\hat{L}_i(d', t)$ on a proxy event day is considered. That is, an ideal load reduction is $\sum_{t \in \mathcal{P}} \left(L_i(d', t) - \hat{L}_i(d', t) \right)$, while the CBL method estimated load reduction is $\sum_{t \in \mathcal{P}} \left(\mathrm{CBL}_i(d', t) - \hat{L}_i(d', t) \right)$. Following the rebate payment rules of Eq. (6.6) and Eq. (6.7), the program-level payment error, which is the sum of the rebate payment

---

[1]Consumption above baseline was not penalized.

error of all customers, is calculated as

$$PE = \sum_{i \in \mathcal{I}} \left(\hat{R}_i - R_i \right), \tag{6.11}$$

where, again, R_i is the ideal rebate, and $\hat{R}_i$ is the estimated rebate. A positive PE indicates a program-level overpayment of rebates by the DR operator. There is an underpayment of rebates to customers when PE is negative. In both cases of overpayment and underpayment, the farther from zero, the worse.

6.3.2   Demand Reduction Cost

The literature is rife with the CBL estimation aspects of DR. However, only a few reports exist on the cost of a DR program, especially from the view of PTR demand reduction. Next, I evaluate the impacts of various CBL estimated methods on the Demand Reduction Cost (DRC) in a DR program.

Following the DPR structure where rebates are paid to customers and the study in [36], I approach the concept of DRC from the perspective of program-level PTR reduction. Therefore, the DRC represents the cost of PTR reductions. The unit of the DRC is $/kW-year [36, 3] when multiple DR programs in a year are jointly evaluated, and $/kW when a DR is singly considered.

Similar to the approach for CBL accuracy evaluation, each of the three events is evaluated separately. I use the DRC, with unit $/kW, to assess rebate payments to customers that participated in each DR program. Simply put, the DRC of x/kW is the x amount of dollars in the loss (cost) incurred for demand reduction estimated with the baseline predicted by a given CBL method.

It is noteworthy that the evaluation of the DRC computed in this work only considers the rebate cost. Other actual costs associated with a DR event include cost procured from DR program start-up, management, campaigns, event notification, and other related activities. Similar to the study in [36], the non-rebate costs are ignored

in the DRC metric due to the non-availability of information on those costs. Since the focus of this work is to compare the DRCs of different CBL methods, the rebate cost information suffices. Similar to the payment error evaluation, the counterfactual demand $\hat{L}_i(d', t)$ on a proxy day is used to assess the DRC in this work.

The DRC is computed as

$$DRC = N_{\mathcal{P}} \left(\frac{\sum_{i \in \mathcal{I}} \hat{R}_i}{\sum_{i \in \mathcal{I}} \sum_{t \in \mathcal{P}} \left(\text{CBL}_i(d', t) - \hat{L}_i(d', t) \right)} \right), \qquad (6.12)$$

where $\sum_{t \in \mathcal{P}} \left(\text{CBL}_i(d', t) - \hat{L}_i(d', t) \right)$ is the CBL estimated load reduction for the ith customer, $\hat{R}_i$ is the paid rebate, and $N_{\mathcal{P}}$ is the total duration, in hours, of the DR event. The higher magnitude of the value, the worse. In addition, a negative value emanates from a total peak event actual consumption being higher than the baseline. A negative DRC means the demand reduction cost is incurred despite not having load reduction at the peak period. The higher the magnitude of a negative DRC, the worse.

6.4   Implementation

The proposed MODWPT-based clustering is applied to the conventional methods to provide improved customer baselines and incentive payment accuracy. Figure 6.1 illustrates the building blocks of the implementation and evaluation of the proposed method.
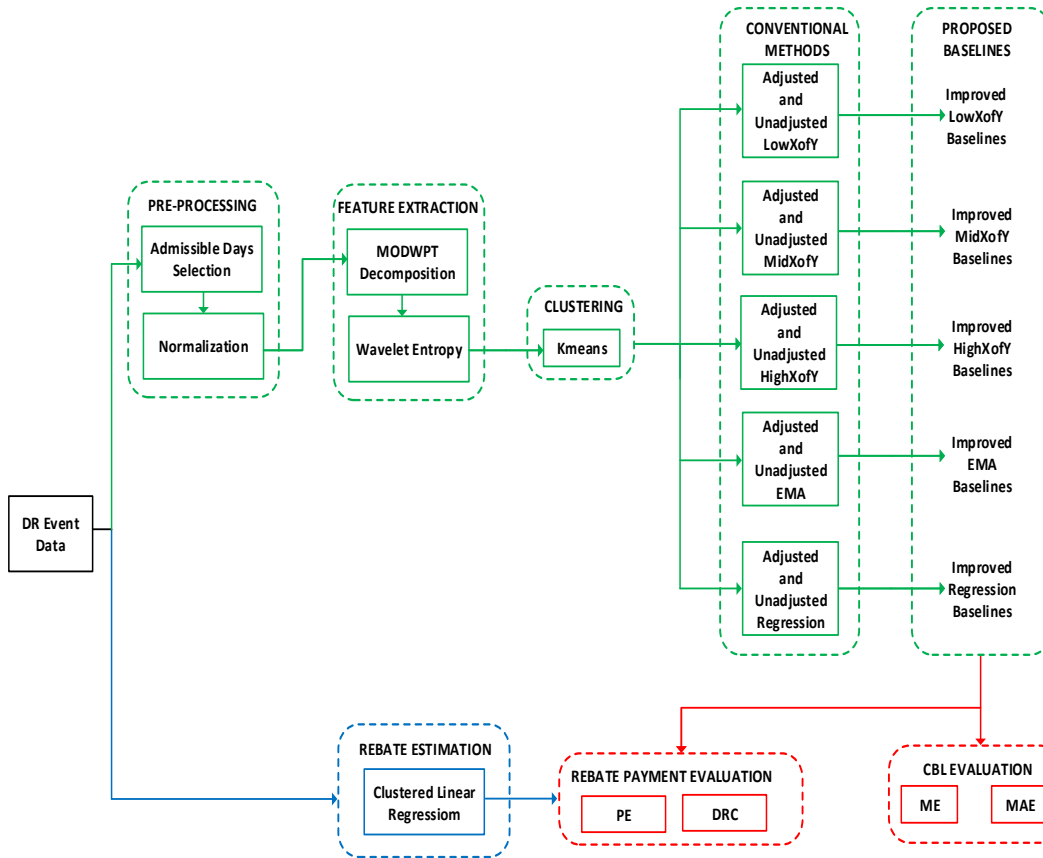
Figure 6.1: Block diagram showing the tasks implemented in this work. The green part is the proposed CBL method presented in Chapter 3. The application of clustered linear regression for the estimation of DR rebates, presented in Chapter 5, is the blue section. The red section of the block diagram delineates the CBL error performance evaluation and the computation of the demand reduction cost, and are presented in this Chapter.

6.4.1   Pre-Processing

The consumption profiles of the customers who enrolled in the DPR tariff were extracted from the Electricity Use Interval Reading data. Leveraging the advantage of MODWPT of the flexibility of starting a time-series data at any point, the most recent quarter data is used for analyzing each DPR DR event. The MODWPT approach to time-series prediction is less susceptible to how far back the "look-back" period can be. Given the non-uniform pattern in the customers' subscription and withdrawal from the programs, the most recent 3-month data preceding each event

most reliably captured consistent customers who participated in the DR event day.

6.4.2   Admissible days selection

One of the primary considerations in CBL estimation is the determination of program-eligible days. The "similar" days to the event day used for the baseline estimation process are referred to as the Admissible days. Similarity, in most cases, is based on the day type. For instance, a non-holiday weekday is a similar day to a weekday DR event day. Admissible days were selected from the historical consumption data preceding the corresponding DR event day. Since all the three programs are weekday DR events, admissible days selected for all CBL estimation methods were weekdays that were neither holidays nor prior event days.

The time-series data comprising the admissible days, for each household participating in a DR event, was normalized. The min-max normalization was employed to scale the data in range $[0, 1]$ as

$$x_{i,norm} = \frac{x_i - \min(X)}{\max(X) - \min(X)},\tag{6.13}$$

where x_i is the ith electricity consumption observation and X denotes the vector of all the observations.

6.4.3   Feature Extraction and Clustering

The proposed CBL estimation by feature extraction entails MODWPT decomposition on the normalized vector of consumption observations in the admissible days for each household. From the original 30-minute interval electricity consumption data, I obtained the sampling frequency f_s of 55.56 microHZ. A 4-level MODWPT was selected, which decomposes the frequency interval $\left[0, \frac{55.56}{2}\mu\text{Hz}\right]$ into 16 equal width intervals. For node $n = 0, \cdots, 2^4 - 1$ in the 4th decomposition level, each node is associated with the frequency interval $\frac{f_s}{32}[n, n+1]$, where f_s is 55.56 microHZ.

The wavelet energy for each signal (household consumption) was obtained from the
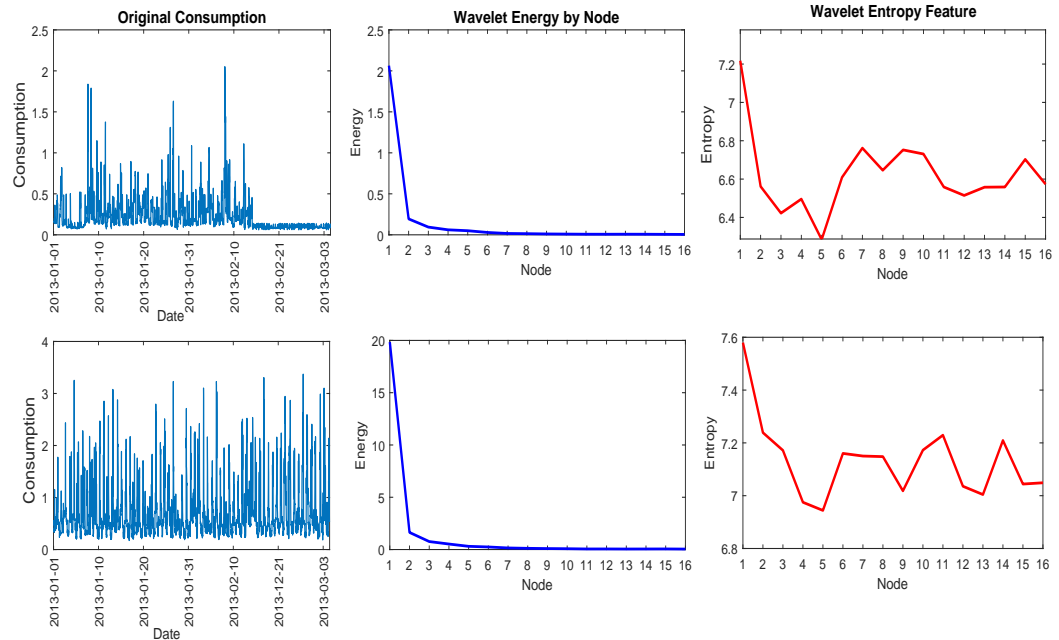
Figure 6.2: The extraction of wavelet energy and entropy features from MODWPT decomposition for two different customers. Household IDs 8147803 (top) and 8664162 (bottom). The wavelet energies in the two homes differ significantly in nodes 1 to 6. The entropy at all nodes differ.

decomposition, as in Eq. (3.7) and Eq. (3.8). Subsequently, the wavelet entropy was extracted, as in Eq. (3.9) and Eq. (3.10). Figure 6.3 shows the wavelet energy and entropy features obtained from 4th level MODWPT decomposition for households with IDs 8147803 and 8664162.

A 1×16 wavelet entropy vector was obtained for each household. The stacked vectors for all households formed a matrix to be used for clustering. A well-known K-means algorithm with Elbow method was used to cluster the households into different unique groups.

Finally, the CBL for each group was computed as the average of the CBL of the members of the group. The group CBL was computed with the conventional CBL estimation methods. The conventional techniques used as benchmarks are Low5of10, Mid4of6, High5of10, EMA, and Regression. For the conventional benchmark methods, the CBL was directly computed from the time domain consumption data. How-

ever, in the case of DFT-based clustering method, CBL was computed based on the performance index described in Eq. (2.8) obtained from DFT of the consumption signal.

6.5 CBL Estimation Results and Discussion

As shown in chapter 3, the proposed MODWPT-based clustering is intended to improve the conventional methods. In the evaluation results presented, the clustering-based CBL estimation methods are described in terms of the conventional methods they are applied to. For example, *Low5of10 with DFT-based clustering* implies an improved Low5of10 achieved by the application of DFT-based clustering to the Low5of10 method. Similarly, *Low5of10 with proposed method* means an improved Low5of10 obtained by the application of the proposed MODWPT-based clustering to the conventional Low5of10 method. For the purpose of comparative analysis, the results from unadjusted conventional methods are presented as benchmarks.

The results presented here show the performance of the CBL methods in the selected DR events. Each event is treated independently and separately. Since the conditions (season, number of participants, etc.) of each are unique, the intent of the metrics is not to compare events. Instead, the focus is on CBL methods.

In the results presented in Tables 6.2 - 6.4, the *Unadj.*, *A.Adj.* and *M.Adj.* represents the adjusted, additively adjusted, and multiplicatively adjusted baselines, respectively. To appropriately compare two CBL methods, it is imperative to compare the results of the same (un)adjusted form. For example, additively adjusted conventional Low4of5 which can be compared with additively adjusted Low4of5 Improvement by DFT clustering.

The ME provides the measure of CBL bias. A positive ME means a CBL method overestimates the baseline, and a negative ME implies an overestimation of the baseline. The closer to zero, the better. The MAE measures the accuracy of a CBL method. Closer to zero indicates a more accurate CBL. The results of the OPI metric

are presented in Figures 6.3 - 6.5. OPI provides a single metric for evaluating a CBL estimation performance. Next, the results are discussed.

Table 6.2: The performance metrics of CBL estimation methods for event I

| Baseline | Mean Error | | | | | | | | |
| | Conventional Baseline | | | DFT Clustering | | | Proposed MODWPT | | |
	Unadj.	A.Adj.	M.Adj.	Unadj.	A.Adj.	M.Adj.	Unadj.	A.Adj.	M.Adj.
Low4of5	-0.0221	-0.0122	0.0049	0.0003	0.0013	0.001	0.0011	-0.001	-0.001
Mid4of6	0.0019	-0.0002	0.0205	0.0178	0.0129	0.0119	0.0164	0.0102	0.0098
High5of10	0.1001	0.0709	0.0849	0.0649	0.0588	0.0568	0.0612	0.0576	0.0568
EMA	0.0223	0.0238	0.0314	0.023	0.0256	0.0247	0.0229	0.0244	0.0246
Regression	0.0312	0.0135	0.09	0.0056	0.0053	0.0055	0.0013	0.0019	0.0018
	Mean Absolute Error								
Low4of5	0.1331	0.1604	0.1652	0.0223	0.0245	0.023	0.0064	0.0074	0.0076
Mid4of6	0.1418	0.1695	0.173	0.0341	0.0304	0.0284	0.0164	0.0102	0.0098
High5of10	0.1952	0.2079	0.2084	0.0752	0.0713	0.069	0.0612	0.0576	0.0568
EMA	0.1438	0.1619	0.1644	0.0379	0.0407	0.0396	0.0229	0.0244	0.0246
Regression	0.2139	0.2129	0.2747	0.0336	0.0376	0.0384	0.0092	0.0086	0.0086

Table 6.3: The performance metrics of CBL estimation methods for event II

Baseline	Mean Error								
	Conventional Baseline			DFT Clustering			Proposed MODWPT		
	Unadj.	A.Adj.	M.Adj.	Unadj.	A.Adj.	M.Adj.	Unadj.	A.Adj.	M.Adj.
Low4of5	-0.1171	-0.0961	-0.0803	-0.1063	-0.0841	-0.0798	-0.1124	-0.0899	-0.0903
Mid4of6	-0.1078	-0.0947	-0.0767	-0.0966	-0.0855	-0.0813	-0.0967	-0.0846	-0.0845
High5of10	-0.0388	-0.0557	-0.04	-0.0783	-0.0748	-0.0733	-0.0787	-0.0736	-0.0734
EMA	-0.0796	-0.0725	-0.0664	-0.0831	-0.0734	-0.0711	-0.0898	-0.0784	-0.078
Regression	-0.0945	-0.0892	-0.0688	-0.0789	-0.0575	-0.0552	-0.0853	-0.0656	-0.0656
	Mean Absolute Error								
Low4of5	0.1979	0.2246	0.2222	0.1132	0.0943	0.0902	0.1124	0.0899	0.0903
Mid4of6	0.1989	0.2259	0.2223	0.1042	0.0952	0.0916	0.0967	0.0846	0.0845
High5of10	0.2019	0.2251	0.2204	0.08	0.0755	0.0742	0.0787	0.0736	0.0734
EMA	0.1933	0.2102	0.2074	0.0945	0.0831	0.0804	0.0898	0.0784	0.078
Regression	0.2453	0.2555	0.2741	0.1001	0.0799	0.0774	0.0853	0.0656	0.0656

Table 6.4: The performance metrics of CBL estimation methods for event III

Baseline	Mean Error								
	Conventional Baseline			DFT Clustering			Proposed MODWPT		
	Unadj.	A.Adj.	M.Adj.	Unadj.	A.Adj.	M.Adj.	Unadj.	A.Adj.	M.Adj.
Low4of5	-0.0489	-0.0351	0.0559	-0.019	-0.0279	-0.0362	-0.0162	-0.026	-0.0362
Mid4of6	0.0109	0.0022	0.093	-0.0193	-0.0683	-0.089	-0.0155	-0.0252	-0.0353
High5of10	0.1292	0.0595	0.0473	0.0485	-0.0091	-0.0541	0.0574	0.027	-0.0073
EMA	0.0166	-0.0101	-0.0384	0.0082	-0.0251	-0.0577	0.0003	-0.0277	-0.055
Regression	-0.0884	-0.2165	-0.1597	-0.0071	-0.0154	-0.0004	0.0017	-0.0018	-0.0066
	Mean Absolute Error								
Low4of5	0.2986	0.333	0.4632	0.0589	0.0692	0.089	0.0265	0.0307	0.0395
Mid4of6	0.309	0.3405	0.4881	0.073	0.1121	0.1461	0.027	0.0311	0.0399
High5of10	0.3501	0.3631	0.457	0.0764	0.0878	0.1201	0.058	0.0351	0.029
EMA	0.3032	0.3202	0.3995	0.0627	0.0703	0.1028	0.0305	0.0377	0.0593
Regression	0.6296	0.5457	0.4923	0.0799	0.0886	0.1283	0.0269	0.0151	0.0261

6.5.1   Effects of CBL Adjustment

Tables 6.2 - 6.4 show the application of the three metrics to CBL estimation methods and their additively and multiplicatively adjusted variants. A table is devoted to each DR event. For most of the results, additive adjustment improves (with closer to zero value) the ME performance of the conventional baselines. With the exception of EMA and Regression of the event I, High5of10 of event II, and Regression of event III, all additive adjustment improves the ME of conventional baselines. However, the instances of improvement to the MEs conventional CBLs by multiplicative adjustment are not more than scenarios with worse-off MEs. For example, multiplicatively adjusted forms of Mid4of6, EMA, and Regression of Event I have worse MEs than their conventional forms. The same performance is observed in MEs of High5of10 of the event I; and all conventional baselines of event II, except High5of10. Therefore, the adjustments (additive and multiplicative) do not definitively improve the performance of the MEs of the conventional baselines. In addition, no adjustment form completely outperforms the other in all the events.

Adjustment improves the ME performance of most of the clustering methods (DFT-based and the proposed). The ME of all adjusted forms (both additive and multiplicative) outperform the unadjusted forms in events I and II, except in clustered EMA of the event I. However, only multiplicatively adjusted form of Regression with DFT and High5of10 with proposed MODWPT have better MEs than their adjusted forms. Thus, adjustments do not absolutely guarantee an improvement of the MEs of the clustering methods. There is also no relatively better performing adjustment between multiplicative and additive adjustments with respect to the ME results.

The unadjusted form of conventional baselines yielded superior MAEs than their adjusted forms, except for additively adjusted Regression of event I and multiplicatively adjusted Regression of event III. On the other hand, the unadjusted form of the clustering methods have higher accuracy than the adjusted forms, save for EMA and

DFT-based Regression of event I; Low4of5, mid4of6, EMA DFT-based High5of10 and MODWPT-based Regression of event II. Therefore, the adjustment does not definitively improve the accuracy of the clustered method. OPI results from Figures 6.3 - 6.5 also confirm that adjustments do not guarantee the improvements of the error metrics.

6.5.2   Comparative Analyses of the CBL methods

The comparison here is made between two CBL methods of the same (un)adjusted form. As delineated in Tables 6.2 - 6.4 and in Figures 6.3 - 6.5, the clustering-based (DFT-based and proposed MODWPT method) methods significantly outperform the traditional CBL methods in terms of accuracy and the overall performance. Specifically, the clustering-based methods yield higher accuracy (MAE) in all 3 DR events. Although there are some instances where the traditional methods yield relatively better bias, the MAEs and the OPIs from the clustering-based methods are significantly much better. It can be concluded from the results that clustering-based methods provide better overall performance than the traditional methods.

In comparing the DFT-based clustering method to the proposed MODWPT method, an "apples-to-apples" comparison is made for clarity. An analogy is made between the unadjusted clustering methods, and a separate comparison is made between each of the adjusted forms. The unadjusted proposed MODWPT method outperforms the unadjusted DFT-based clustering in all the events. Similarly, the overall performance of the adjusted forms of the proposed also exceeds those of the DFT-based.
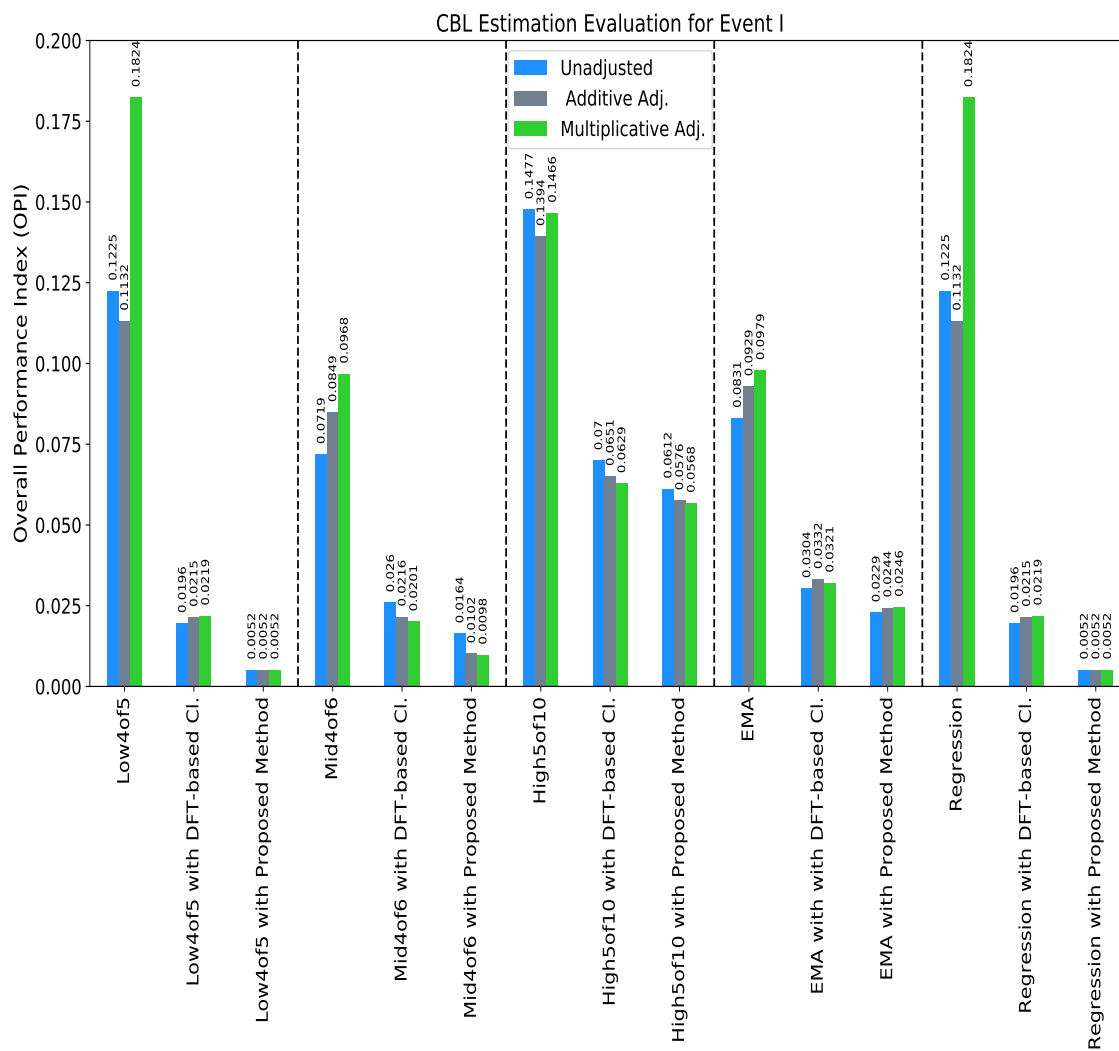
Figure 6.3: Error performance of CBL estimation methods for event I.
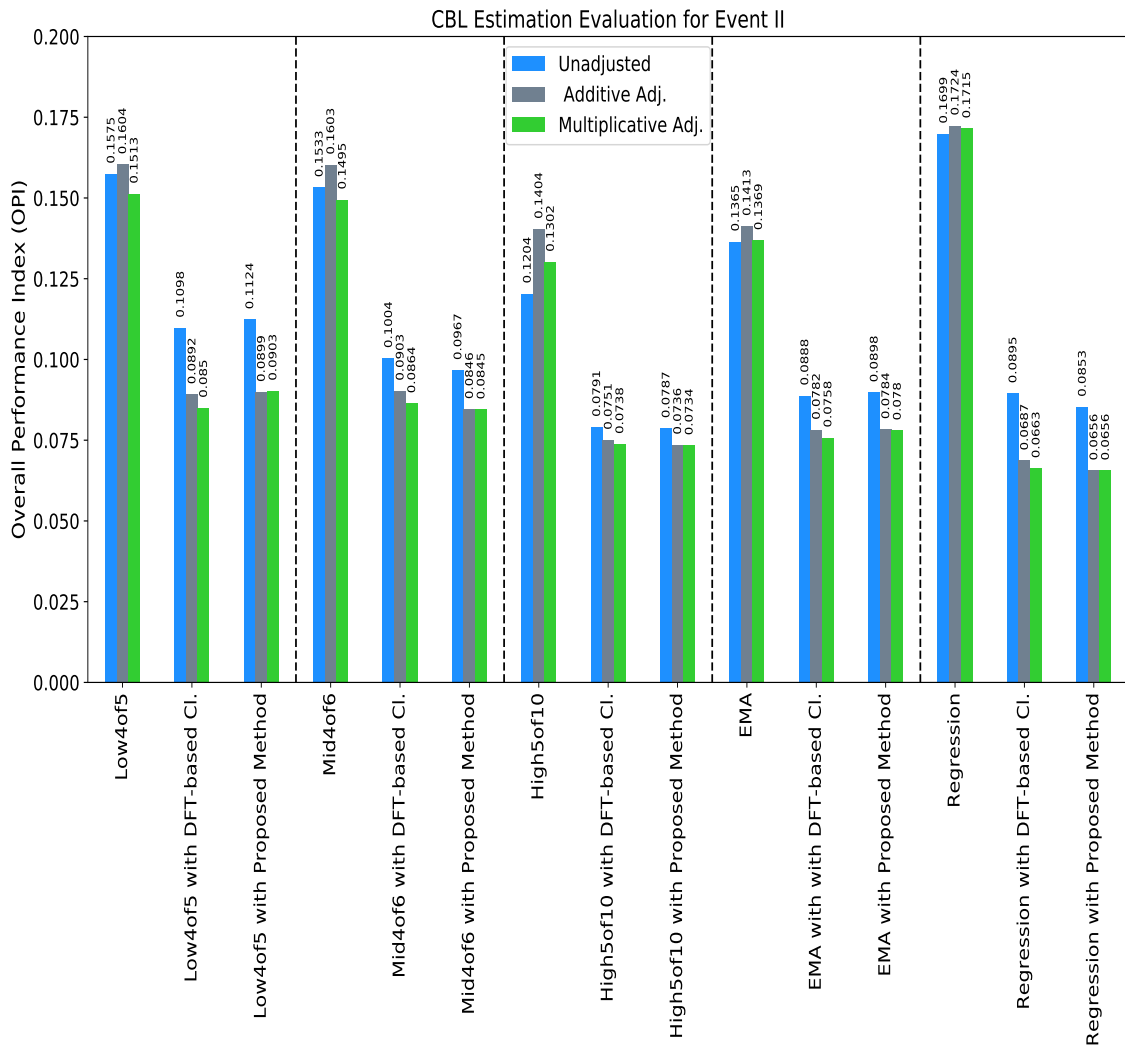
Figure 6.4: Error performance of CBL estimation methods for event II.
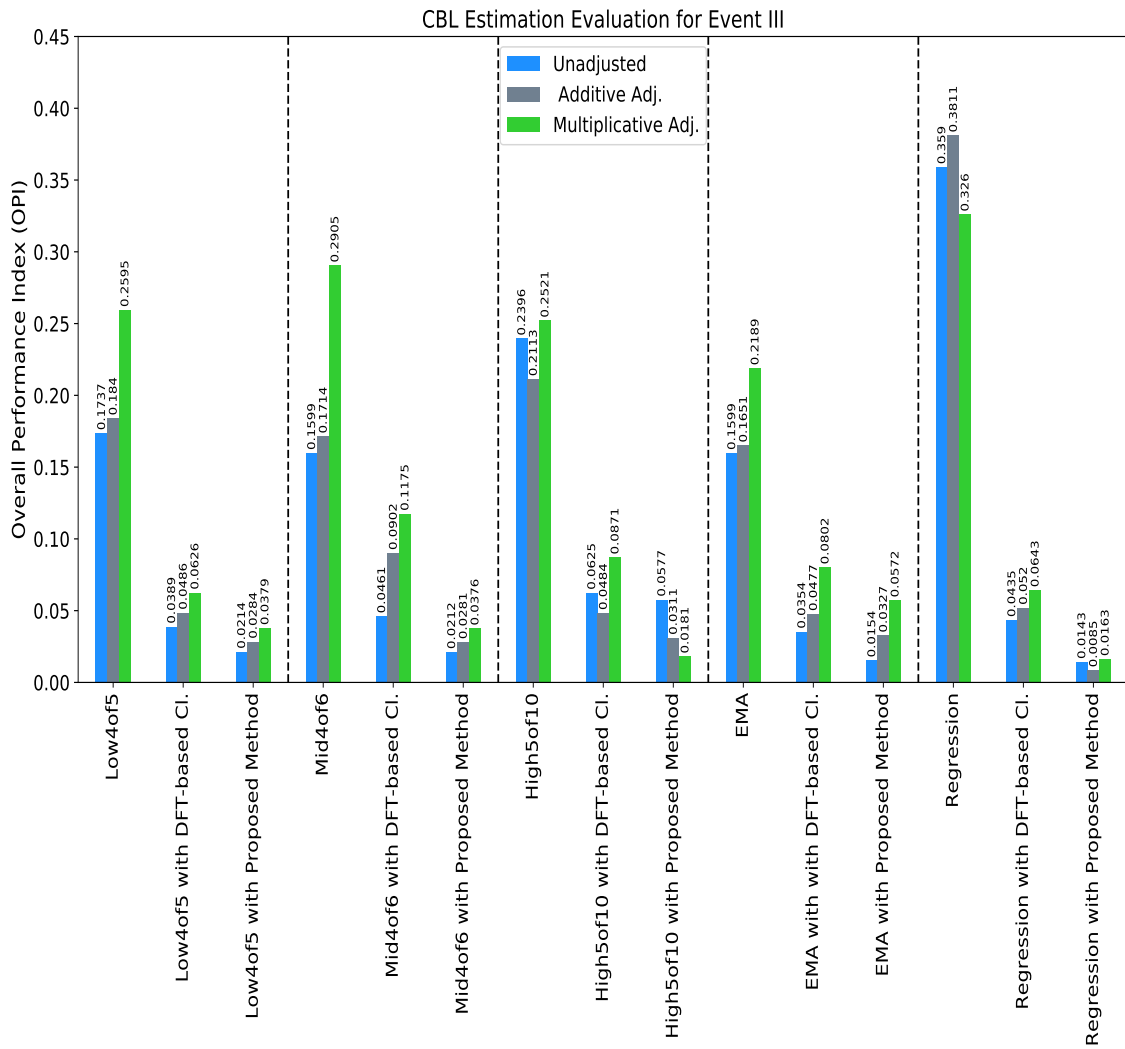
Figure 6.5: Error performance of CBL estimation methods for event III.

6.6 Rebate Payment Results and Discussion

6.6.1 Payment Error Results and Discussion

The payment errors (PEs) in the three selected events are shown in Table 6.5 - 6.7. A positive PE denotes an overpayment of the total rebate paid to the customers, whereas an underpayment of the total rebate is indicated by a negative PE. The larger the PE, the higher the errors from incentive payment.The closer to zero, the better the PE. The conventional baselines resulted in higher positive payment errors than clustering methods. And the proposed method yielded lower PEs than the DFT-base clustering method. In fact, there are some scenarios where the proposed method gives zero PE, for example, all baselines of event II. It can also be observed from the results that the adjusted methods do not guarantee a reduction in PEs in all baselines.

6.6.2 Demand Reduction Cost Results and Discussion

The DRCs are computed for the case study DR events. For comparative analysis, DRCs are calculated from multiple baselines estimated from the benchmarks and the proposed CBL methods. A rebate estimate, obtained from clustered linear regression, is computed using the peak time load reduction values from each CBL method. The DRC values represent the cost of procuring demand reductions through DR programs from rebate payment.

A DRC can either be positive or negative. A positive value is more desirable than a negative value. As evident from Eq. (6.5), a large total load reduction would yield a low DRC value. Thus, a lower positive value indicates a better DRC. From the denominator of the DRC formula, a negative DRC value indicates the aggregate load reduction is negative since $\hat{R}_i$ is either positive or zero, and $N_{\mathcal{P}}$ is always positive. The higher the deviation from zero, the worse the negative DRC value.

Tables 6.5 - 6.7 present the DRC values for the DR events. Adjusted forms of CBL do not definitively improve the DRC values of the peak time load reduction.

The DFT-based clustering method provides better DRC values, when positive than the traditional CBL methods in all the events. The proposed MODWPT method provides the lowest DRCs for PTR demand reduction in all the events. Similarly, the adjusted form of the proposed MODWPT method also has lower DRCs than the adjustment of other baselines. Therefore, the proposed MODWPT method gives the lowest cost of achieving load reduction through a dynamic peak rebate DR program.

Table 6.5: Assessment of rebate payment for DR load reduction for event I.

Baseline	Payment Error[Aus$]								
	Conventional Baseline			DFT Clustering			Proposed MODWPT		
	Unadj.	A.Adj.	M.Adj.	Unadj.	A.Adj.	M.Adj.	Unadj.	A.Adj.	M.Adj.
Low4of5	1174.07	1839.03	1932.54	176.63	270.14	218.19	41.56	-31.17	-41.56
Mid4of6	1350.7	1963.71	2244.24	748.08	644.18	581.84	613.01	384.43	363.65
High5of10	3937.81	3459.87	3730.01	2441.65	2275.41	2171.51	2285.8	2150.73	2119.56
EMA	1568.89	2026.05	2181.9	924.71	1070.17	1018.22	851.98	914.32	914.32
Regression	2909.2	2846.86	5101.49	509.11	706.52	727.3	0	0	0
	Demand Reduction Cost[Aus$/kW]								
Low4of5	-38.34	-385.28	41.21	19.58	23.56	21.61	16.51	17.34	17.32
Mid4of6	34.17	58.12	27.91	16.69	18.03	17.74	16.1	16.29	16.3
High5of10	16.26	18.17	17.29	15.94	16.13	16.08	15.88	15.89	15.9
EMA	20.29	22.99	21.37	16.37	16.7	16.62	16.01	16.03	16.03
Regression	25.19	37.53	21.03	-28.38	57.73	56.14	0	0	0

Table 6.6: Assessment of rebate payment for DR load reduction for event II.

Baseline	Payment Error[Aus$]								
	Conventional Baseline			DFT Clustering			Proposed MODWPT		
	Unadj.	A.Adj.	M.Adj.	Unadj.	A.Adj.	M.Adj.	Unadj.	A.Adj.	M.Adj.
Low4of5	736.47	1811.95	2104.2	46.76	140.28	-46.76	0	0	0
Mid4of6	970.27	1882.09	2045.75	58.45	128.59	140.28	0	0	0
High5of10	923.51	1706.74	1624.91	-1005.34	-771.54	-736.47	-1005.34	-771.54	-736.47
EMA	1320.97	1998.99	1928.85	-23.38	128.59	116.9	0	0	0
Regression	2104.2	2478.28	3530.38	93.52	198.73	198.73	0	0	0
	Demand Reduction Cost[Aus$/kW]								
Low4of5	-1.86	-6.01	-10.59	-0.12	-0.61	-0.71	0	0	0
Mid4of6	-2.89	-6.5	-12.44	-0.22	-0.54	-0.62	0	0	0
High5of10	81.93	-43.23	273.44	-0.02	0	0	0	0	0
EMA	-7.72	-11.59	-15.03	-0.43	-0.65	-0.63	0	0	0
Regression	-6.13	-7.65	-20.01	-0.14	-0.53	-0.56	0	0	0

Table 6.7: Assessment of rebate payment for DR load reduction for event III.

Baseline	Payment Error[Aus$]								
	Conventional Baseline			DFT Clustering			Proposed MODWPT		
	Unadj.	A.Adj.	M.Adj.	Unadj.	A.Adj.	M.Adj.	Unadj.	A.Adj.	M.Adj.
Low4of5	1048.32	1670.4	3813.12	-483.84	-714.24	-748.8	-495.36	-794.88	-1117.44
Mid4of6	1751.04	2188.8	4803.84	-541.44	-1670.4	-1589.76	-472.32	-771.84	-1082.88
High5of10	4250.88	3110.4	3813.12	1520.64	-230.4	-1117.44	1785.6	840.96	-218.88
EMA	1589.76	1612.8	2407.68	288	-645.12	-1221.12	23.04	-852.48	-1635.84
Regression	6186.24	3006.72	3144.96	817.92	576	1416.96	403.2	0	138.24
	Demand Reduction Cost[Aus$/kW]								
Low4of5	55.77	30.33	14.31	11.84	12.13	13.01	11.45	11.46	11.49
Mid4of6	15.64	18.16	13.61	11.61	16.24	31.1	11.44	11.46	11.51
High5of10	11.54	13.33	15.03	11.33	11.55	15.7	11.31	11.33	11.37
EMA	14.02	18.19	28.25	11.43	12.04	18.21	11.38	11.48	12.76
Regression	-13.3	-2.99	-2.36	-16.04	-3.48	-6.88	77.14	0	-0.76

CHAPTER 7: CONCLUSION AND FUTURE WORKS

7.1   Conclusion

In this thesis, it is emphasized that an accurate estimation of CBL is a key element in the successful implementation of DR, especially for residential customers where there is large randomness in energy consumption. In order to calculate the decrease in demand in DR programs, it is crucial to accurately estimate the consumption baselines at the designated peak periods. This thesis sought to improve the accuracy of the conventional baseline estimation methods by proposing a novel clustering-based CBL method, which leverages wavelet entropy features extracted from the maximal overlap discrete wavelet packet transform (MODWPT) decomposition. To compare the error performance of the proposed method with the traditional CBL methods, some dynamic peak rebate (DPR) demand response programs were used as the case study. The rebate payment in the DR programs was determined by Clustered Linear Regression with high R-squared accuracy. Furthermore, demand reduction costs of the PTR demand reduction, from using different CBL estimation methods, were computed. It was shown that the proposed MODWPT method provided the lowest demand reduction costs compared to all the benchmark methods, in all the DR events.

The key conclusions are:

- The MODWPT variant of wavelet packet transform is chosen for its non-sensitivity to the starting point of a time-series data. Also, MODWPT provides higher resolution, due to the decomposition of its both low and high frequency coefficients, than conventional (discrete) wavelet transform.

- The wavelet energy and entropy features of MODWPT decomposition contain

underlying features with which households can be clustered using their time-series energy consumption profile.

- The formulas used to compute the rebate payment in the DPR demand response programs were not revealed by the operators. Clustered Linear Regression was performed on the DR events data to obtain the rebate paid with high R-squared accuracy.

- The DFT-based clustering CBL estimation proposed in [38] was originally evaluated with a proxy DR event. In this thesis, actual DR events were used to compare its error performance. The results of this thesis corroborate the superior error performance of the DFT-based clustering method over the traditional CBL estimation methods.

- The overall performance index (OPI) of clustering-based methods significantly outperforms that of the traditional CBL methods. Moreover, the proposed MODWPT method shows superior OPI performance over the DFT-based clustering technique.

- CBL adjustment does not definitively improve the OPIs of customer baselines estimation, although adjustment has a higher likelihood of improving the MAE than the ME.

- The demand reduction costs is a metric for comparing the cost of achieving load reductions via a DR to the cost of procuring capacity from alternative energy sources. The proposed MODWPT method shows much better demand reduction costs than both the traditional and DFT-based clustering CBL methods.

7.2   Future Works

Based on the results of this thesis and the available related data, some directions for future works are suggested as follows.

- An investigation can be conducted on the behavioral changes of customers before and during a DR event. As noted in section 4.1, appliances were controllable (switched on or off) using smart plugs via an online portal or a mobile device. The setup is referred to as the *Home Area Network (HAN)*. The HAN data for the SGSC program is also available in the data source [32], where energy consumption data is obtained for this thesis. The time-series data of operation times of appliances such as microwave, television, dishwater, electric kettle, washing machine, fridge, and air-conditioner are provided. It would be an interesting research to study if the customers exhibited strategic behaviors in the days prior to the DR events in a way to affect baseline computation.

- It will be insightful to study the impacts of electric vehicles (EVs) on peak demand. The charging regimes of an electric vehicle add load to a customer's consumption profile. A DR event data containing an EV's separate contribution to each customer's electricity demand can be sourced to investigate the impact of electric vehicles on peak demand.

REFERENCES

[1] Kathleen Spees. *Meeting electric peak on the demand side: Wholesale and retail market impacts of real-time pricing and peak load management policy.* PhD thesis, Carnegie Mellon University, 2008.

[2] D Wight et al. 2010 assessment of demand response and advanced metering staff report. *Federal Energy Regulatory Commission, USA*, 2011.

[3] Ryan Hledik and Ahmad Faruqui. Valuing demand response: International best practices, case studies, and applications. *Prepared for EnerNOC*, 2015.

[4] Chen Chen, Jianhui Wang, and Shalinee Kishore. A distributed direct load control approach for large-scale residential demand response. *IEEE Transactions on Power Systems*, 29(5):2219–2228, 2014.

[5] Mahmood Hosseini Imani, Milad Yousefi Talouki, Payam Niknejad, and Kamran Yousefpour. Running direct load control demand response program in microgrid by considering optimal position of storage unit. In *2018 IEEE Texas Power and Energy Conference (TPEC)*, pages 1–6. IEEE, 2018.

[6] Cynthujah Vivekananthan, Yateendra Mishra, Gerard Ledwich, and Fangxing Li. Demand response for residential appliances via customer reward scheme. *IEEE transactions on smart grid*, 5(2):809–820, 2014.

[7] Peter Schwarz, Saeed Mohajeryami, and Valentina Cecchi. Building a better baseline for residential demand response programs: Mitigating the effects of customer heterogeneity and random variations. *Electronics*, 9(4):570, 2020.

[8] *Common Demand Response Practices and Program Designs*, (accessed April 12, 2020). https://www.michigan.gov/documents/energy/ Common_Practices_Feb22_522983_7.pdf.

[9] Chen-Ching Liu, Stephen McArthur, and Seung-Jae Lee. *Smart grid handbook, 3 volume set.* John Wiley & Sons, 2016.

[10] M Norris, R Cliff, R Sharp, S Koci, and H Gardner. Smart grid, smart city: Shaping australia's energy future national cost benefit assessment. *Arup, Report*, 2014.

[11] Nathan Walsh. Residential electricity usage: How do households respond to dynamic peak pricing events? Master's thesis, School of Economics, University of New South Wales, 2016.

[12] Tri Kurniawan Wijaya, Matteo Vasirani, and Karl Aberer. When bias matters: An economic assessment of demand response baselines for residential customers. *IEEE Transactions on Smart Grid*, 5(4):1755–1763, 2014.

[13] Seungman LEE. Comparing methods for customer baseline load estimation for residential demand response in south korea and france: Predictive power and policy implications. 2019.

[14] Saeed Mohajeryami, Milad Doostan, and Peter Schwarz. The impact of customer baseline load (CBL) calculation methods on peak time rebate program offered to residential customers. *Electric Power Systems Research*, 137:59–65, 2016.

[15] Yi Zhang, Weiwei Chen, Rui Xu, and Jason Black. A cluster-based method for calculating baselines for residential loads. *IEEE Transactions on smart grid*, 7(5):2368–2377, 2015.

[16] Shunfu Lin, Fangxing Li, Erwei Tian, Yang Fu, and Dongdong Li. Clustering load profiles for demand response applications. *IEEE Transactions on Smart Grid*, 10(2):1599–1607, 2017.

[17] Xu Chen and Andrew N Kleit. Money for nothing? why ferc order 745 should have died. *The Energy Journal*, 37(2), 2016.

[18] Hung-po Chao. Demand response in wholesale electricity markets: the choice of customer baseline. *Journal of Regulatory Economics*, 39(1):68–88, 2011.

[19] Donald B. Percival and Andrew T. Walden. *Wavelet Methods for Time Series Analysis*. Cambridge University Press, 2000.

[20] Eunjung Lee, Dongsik Jang, and Jinho Kim. A two-step methodology for free rider mitigation with an improved settlement algorithm: Regression in CBL estimation and new incentive payment rule in residential demand response. *Energies*, 11(12):3417, 2018.

[21] Saeed Mohajeryami. An investigation of the impact of customer baseline (CBL) calculation on peak time rebate program. Master's thesis, University of North Carolina at Charlotte, 2016.

[22] Saeed Mohajeryami, Roozbeh Karandeh, and Valentina Cecchi. Correlation between predictability index and error performance in customer baseline load (CBL) calculation. In *2017 North American Power Symposium (NAPS)*, pages 1–6. IEEE, 2017.

[23] Miriam L Goldberg and G Kennedy Agnew. Measurement and verification for demand response. *US Department of Energy: Washington, DC, USA*, 2013.

[24] Tianli Song, Yang Li, Xiao-Ping Zhang, Jianing Li, Cong Wu, Qike Wu, and Beibei Wang. A cluster-based baseline load calculation approach for individual industrial and commercial customer. *Energies*, 12(1):64, 2019.

[25] Saeed Mohajeryami, Milad Doostan, Ailin Asadinejad, and Peter Schwarz. Error analysis of customer baseline load (CBL) calculation methods for residential customers. *IEEE Transactions on Industry Applications*, 53(1):5–14, 2016.

[26] Zhengyou He. *Wavelet analysis and transient signal processing applications for power systems.* John Wiley & Sons, 2016.

[27] Stuart Lloyd. Least squares quantization in pcm. *IEEE transactions on information theory,* 28(2):129–137, 1982.

[28] John MacQueen. Some aspects of the early renaissance in scotland. In *Forum for Modern Language Studies,* volume 3, pages 201–222. Narnia, 1967.

[29] Glenn W Milligan and Martha C Cooper. An examination of procedures for determining the number of clusters in a data set. *Psychometrika,* 50(2):159–179, 1985.

[30] Tadeusz Caliński and Jerzy Harabasz. A dendrite method for cluster analysis. *Communications in Statistics-theory and Methods,* 3(1):1–27, 1974.

[31] Arnis Kirshners, Arkady Borisov, Serge Parshutin, et al. Robust cluster analysis in forecasting task. In *International Scientific Conference: Applied Information and Communication Technologies, 5, Jelgava (Latvia), 26-27 Apr 2012.* [LLU], 2012.

[32] Smart-grid smart-city customer trial data. https://data.gov.au/dataset/ds-dga-4e21dea3-9b87-4610-94c7-15a8a77907ef/details?q=demand%20response%20electricity. Accessed: 2020-01-05.

[33] Bertan Ari and H Altay Güvenir. Clustered linear regression. *Knowledge-Based Systems,* 15(3):169–175, 2002.

[34] Hadley Wickham et al. The split-apply-combine strategy for data analysis. *Journal of Statistical Software,* 40(1):1–29, 2011.

[35] Nathan Walsh and Tess Stafford. Honours thesis. 2016.

[36] S George, J Bode, and D Berghman. San diego gas & electric peak time rebate baseline evaluation. *California Measurement Advisory Council,* 2012.

[37] Eunjung Lee, Kyungeun Lee, Hyoseop Lee, Euncheol Kim, and Wonjong Rhee. Defining virtual control group to improve customer baseline load calculation of residential demand response. *Applied Energy,* 250:946–958, 2019.

[38] Saeed Mohajeryami. *An improvement of the load reduction evaluation methodologies employed in demand response (DR) programs offered to residential customers.* PhD thesis, The University of North Carolina at Charlotte, 2017.